Remote Sensing Study of Mangrove Forest Health and Resilience in the Grand-Pierre Bay, Artibonite, Haiti

Alexandre Erich Sébastien Georges[1], Mark T. Stacey[2], and Deanesh Ramsewak[3]

[1]University of California Berkeley
[2]University of California, Berkeley
[3]The University of Trinidad and Tobago

January 11, 2025

Abstract

As climate change increases the vulnerability of Small Island Developing States' marginalized coastal communities and ecosystems, it is necessary to evaluate the health and resilience of their natural landforms and infrastructure inventories. For example, mangroves could be a central component of coastal adaptation strategies for these sites due to their storm surge attenuating properties. One such forest is located in Haiti in the Grand-Pierre Bay, south of Gonaives and at the mouth of the Artibonite Valley, a region important for its agriculture. A remote sensing study of the Grand-Pierre Bay mangroves was conducted using imagery from PlanetLabs, machine learning tools, and vegetation health indices to identify and track mangrove cover, health, and spatio-temporal changes between 2010 and 2020. Detected changes in cover and NDVI (Normalized Difference Vegetation Index) values display a retreat of mangrove cover from the sea, with most of the retreat and health loss occurring during the 2013-2016 Pan-Caribbean drought, which was also experienced in Haiti. While the forest displays recovery post-drought, health increases and new establishments are concentrated on the landward side of the forest, and continued retreat is occurring on the shoreline, indicating a landward migration of the forest. This migration may, however, not occur fast enough to offset the losses on the coast, and targeted conservation efforts may be required to sustain and enhance the forest's resilience.

Remote Sensing Study of Mangrove Forest Health and Resilience in the Grand-Pierre Bay, Artibonite, Haiti

Alexandre E. S. Georges[1*], Mark T. Stacey[1], Deanesh Ramsewak[2]

[1]University of California, Berkeley
[2]Centre for Maritime and Ocean Studies, The University of Trinidad and Tobago

Key Points:

- The 2013 Pan-Caribbean drought weakened the Grand-Pierre Bay mangrove forest in Haiti. Recovery was uneven, with continued coastal retreat.
- Tide gauge data in Haiti showed local sea-level rises partly coinciding with the Pan-Caribbean drought. This combination of environmental factors likely stressed the mangrove forest, contributing to the observed pattern of coastal retreat and landward migration.
- The forest's landward migration is unsustainable as the available landward space may not support continued mangrove establishment, raising concerns about the long-term resilience of the forest.

[*]H2H8

Corresponding author: Alexandre Georges, alexandre_georges@berkeley.edu

Abstract

As climate change increases the vulnerability of Small Island Developing States' marginalized coastal communities and ecosystems, it is necessary to evaluate the health and resilience of their natural landforms and infrastructure inventories. For example, mangroves could be a central component of coastal adaptation strategies for these sites due to their storm surge attenuating properties. One such forest is located in Haiti in the Grand-Pierre Bay, south of Gonaives and at the mouth of the Artibonite Valley, a region important for its agriculture. A remote sensing study of the Grand-Pierre Bay mangroves was conducted using imagery from PlanetLabs, machine learning tools, and vegetation health indices to identify and track mangrove cover, health, and spatio-temporal changes between 2010 and 2020. Detected changes in cover and NDVI (Normalized Difference Vegetation Index) values display a retreat of mangrove cover from the sea, with most of the retreat and health loss occurring during the 2013-2016 Pan-Caribbean drought, which was also experienced in Haiti. While the forest displays recovery post-drought, health increases and new establishments are concentrated on the landward side of the forest, and continued retreat is occurring on the shoreline, indicating a landward migration of the forest. This migration may, however, not occur fast enough to offset the losses on the coast, and targeted conservation efforts may be required to sustain and enhance the forest's resilience.

Plain Language Summary

As climate change's impact on Small Island Developing States becomes more apparent, evaluating how their natural environments cope is essential. Coastal communities in these states often benefit from natural defenses like mangrove forests for protection against flooding. This study focuses on the Grand-Pierre Bay mangrove forest in Haiti, located south of Gonaives and at the mouth of the Artibonite Valley, a vital agricultural area.

By analyzing satellite images and land cover maps, we tracked changes in the forest's size and health between 2010 and 2020. Results showed the forest was stressed and retreating, with the most loss occurring between 2013 and 2016, coinciding with the Pan-Caribbean drought. While inland areas are recovering, the coastline mangroves continue to decline, indicating landward migration.

We suggest that reduced freshwater input and rising sea levels contributed to this decline. If these current trends continue, this would have serious implications for mangrove resilience and their ability to protect against flooding in this area.

1 Introduction

In the face of escalating climate change impacts worldwide, governments and communities are looking at possible adaptation pathways to mitigate its effects. For Small Island Developing States (SIDS) in the Caribbean, the use of natural landforms such as wetlands in coastal defense infrastructure provides some optimism. Due to increased hurricane activity in the North Atlantic (Murakami et al., 2020), the Caribbean islands are particularly vulnerable to the impacts of climate change on coastlines, with increased flooding due to storm surges being expected as a result. In Haiti, this increased coastal vulnerability disproportionately impacts disadvantaged urban and rural populations and critical economic centers; out of the 10 communes (municipalities) with the largest number of people living in income poverty in 2012 in Haiti, 7 are coastal (Pokhriyal et al., n.d.). Mangrove forests, which are native to the region, may be viable candidates as landforms to be implemented in adaptation strategies in Haiti and the larger Caribbean region.

Experimental and observational studies have shown mangroves' capacity to abate the flooding impacts of storm surges by reducing water elevation and velocity due to drag in their complex root systems. Field observations of storm surges created by Category 3 Hurricane Wilma along the Gulf Coast of South Florida showed effective attenuation of storm surges by the Everglades mangroves, with the surge amplitudes decreasing by a rate of up to 40-50 cm/km across the forest (Zhang et al., 2012). An experiment using scale models of mangroves by Maza et al. (2017) indicates reductions in the velocity field by up to 50 percent and turbulence kinetic energy increases by up to fivefold within the root zone compared to upstream conditions. And while it is hard for numerical simulations to accurately quantify mangrove forests' storm surge attenuation property, hydrodynamic modeling studies have demonstrated their attenuating effect on storm surge amplitudes and flood durations (Montgomery et al., 2019; Chen et al., 2021). Mangroves' ability to restrict water flow across the forest width then leads to reductions in peak water levels, flooding extent, and flood duration in areas within and behind the forest.

At the same time, the degree to which mangroves are effective in providing coastal protection depends on their health and cover, which are influenced by environmental processes. Hydrodynamic properties, such as tidal patterns and hydroperiod, play a role in the propagation and zonation of mangroves (Crase et al., 2013; Salas-Rabaza et al., 2023). Salinity levels, closely linked with hydrodynamics, play an essential role in the well-being of mangroves, as prolonged high salinity exposure may result in restricted growth of trees (Krauss et al., 2008) and has been shown to be the primary contributor behind several mangrove diebacks around the world (Lagomasino et al., 2021; Lovelock et al., 2017). Other identified environmental factors influencing mangrove health include temperature, light, nutrients, and sediment supply. Consequently, climate events like droughts or long-term phenomena such as sea-level rise may threaten mangrove forests' health and resilience.

Before assessing the potential of current mangrove covers in the Caribbean as natural infrastructure, it is essential to evaluate how their recent health has changed due to stressors related to climate and human activities. Remote Sensing tools and techniques are well suited to answer this question as they offer frequent data points on ecosystems and landforms, letting observers track these systems' evolution over time and their response to external factors or events. Examples include the monitoring of crop growth and health (Sadeh et al., 2021) , monitoring the resilience of mangroves to sea level rise (Duncan et al., 2018) and measuring their biophysical characteristics (Jean-Baptiste & Jensen, 2006). Hence the use of satellite imagery has been shown to be appropriate for studying mangroves. Tools such as machine learning and vegetation indices can be used to track the extent and health of mangrove forests over time. Coupled with other climate data, these time series can help us determine the impacts of climate events on these forests.

In this paper, we develop and apply a workflow to assess and track mangrove forest health over the last decade. Satellite images of mangrove forests in Haiti taken between 2010 and 2020 are classified and analyzed to distinguish mangrove covers from other land covers. This lets us measure their extent evolution through indices and metrics that reflect forest health. This analysis then allows us to quantify changes in mangrove health in Haiti, helping us understand the relationship between their resilience and recent climate events.

2 Data and Study Sites

The Grand-Pierre Bay mangrove forest, located at the mouth of the Artibonite Valley, was selected for this study due to its significant size (largest single mangrove extent in Haiti), and proximity to population and economic centers.

Satellite imagery from PlanetLabs' RapidEye archive is used for our analysis. With a 5m pixel resolution, this satellite lets us better distinguish smaller-scale forest cover details than other satellites such as Landsat (30m resolution). PlanetLabs also provides high temporal resolution with near-daily observations, letting us follow seasonal changes in our sites. While featuring fewer bands than Landsat for analysis, the provided 5-band imagery (Red, Blue, Green, RedEdge, and Near-Infrared) is still well-suited to land classification, particularly when used in conjunction with indices such as the Normalized Difference Vegetation Index (NDVI) and the Normalized Difference Water Index (NDWI). As such, intra-annual observations are taken between 2010 and 2020 at the Grand-Pierre Bay site. Cloud cover permitting, several observations are taken in a single month. With a decade-long observation period, we can observe seasonal and inter-annual patterns of mangrove health and cover.

Baie de Grand-Pierre, Haiti (Grand-Pierre Bay)

Figure 1. The Grand-Pierre Bay mangrove forest (outlined in solid white) is located on the Central coastline of Haiti, South of the city of Gonaives. The major rivers' paths (La Quinte, L'Estère and Artibonite) are highlighted. Major settlements are outlined in dashed lines.

The Grand-Pierre Bay Mangrove Forest (outlined in white in Fig.1) is located south of Gonaives, the 3rd most populated city in Haiti, in the Artibonite department. It is the largest single extent of mangroves in Haiti and is fed by the La Quinte and L'Estère rivers, the two most important rivers in this department after the Artibonite River. The mangrove forest sits seaward of a lagoon, acting as a buffer for parts of the Artibonite Valley coastline. Its close proximity to Gonaives and the Artibonite Valley mouth is significant as this region houses one of the largest disadvantaged urban populations of the country, with the commune of Gonaives holding the largest number of people living in income poverty in Haiti in 2012 (Pokhriyal et al., n.d.). The Artibonite Valley is also one of the country's most important agricultural production regions, with over 70 percent of the country's rice production, a local staple, occurring in the valley ("Assessing the Potential Impact of Climate Change on Rice Yield in the Artibonite Valley of Haiti Using the CSM-CERES-Rice Model", n.d.).

Caroni Swamp, Trininad-and-Tobago

Figure 2. Caroni Swamp (outlined in solid white) is located on the Western coast of the island of Trinidad, South of the cities of Port-of-Spain and San Juan.

To ground-truth the analyses that we present below, which focus on Grand-Pierre Bay, we require independent observations of land cover in order to train the land classification model. The primary site providing this data is the Caroni Swamp (outlined in white in Fig. 2), which is located south of the capital city of Trinidad and Tobago, Port-of-Spain. It is the country's largest mangrove wetland, protected under the Ramsar Convention for International Wetland Protection. The swamp is home to numerous channels, lagoons, and intertidal mudflats. Unlike the chosen Haitian sites, the Caroni Swamp is surrounded by highly urbanized areas, with Port-of-Spain and San Juan to the north and Chaguanas to the southeast and built infrastructure backing the mangrove on its landward edge. This site is used for ground-truthing our land classification model.

2.1 Climate Forcing during Observation Period

Rainfall estimates from the Climate Hazards Group InfraRed Precipitation with Station data (CHIRPS) are used to follow climate trends in the Grand-Pierre Bay mangrove forest over our observation period (Fig. 14). CHIRPS is a 35+ year quasi-global rainfall data set which combines interpolated station data and gridded satellite-based precipitation estimates from NASA and NOAA (Funk et al., 2015).

Additionally, tide gauge data from around the island of Haiti/Hispaniola (across Haiti and the Dominican Republic) are used to monitor the local sea level variations (Fig. 15).

3 Methods

Our approach involves using remote sensing indices (defined below) to support the classification of images and the calculation of metrics to be analyzed.

3.1 Indices

Normalized Difference Water Index - NDWI

The Normalized Difference Water Index (NDWI) assesses the presence and extent of surface water bodies. It is used here to mask the open water pixels surrounding the mangrove forest to aid the land classification process. This is done using the Green and Near-Infrared bands, following the relation defined by McFeeters (1996):

$$NDWI = \frac{Xgreen - Xnir}{Xgreen + Xnir}$$

Our land classification and analysis uses the land surfaces obtained after masking out open water using NDWI based on a threshold of 0.2, with values higher than this threshold masked as open water.

Normalized Difference Vegetation Index - NDVI

The Normalized Difference Vegetation Index (NDVI) is a simple indicator of green vegetation's presence, density, and health. This index uses the Near-Infrared and Red bands of observations as follows:

$$NDVI = \frac{Xnir - Xred}{Xnir + Xred}$$

Applied to our mangrove cover after masking it out from other land covers, we gauge the density and health evolution of our mangroves through time series and looking at the spatial difference of NDVI distribution between 2020 and 2010:

$$dNDVI = NDVI_{2020} - NDVI_{2010}$$

3.2 Land Classification using Machine Learning

Unsupervised Learning

Initially, we explored employing unsupervised learning to quickly determine what features and structures can be found and classified from our images and surface reflectance data. The unsupervised classified images helped us familiarize ourselves with the sites' likely covers and distributions. This analysis was conducted using the K-means clustering algorithm, popular for image segmentation (Ikotun et al., 2023). This method initializes k centroids (where k is the user-defined number of clusters). The centroids are then recomputed as the mean of all the data points in the cluster, and the assignment of data points to clusters is repeated until the centroids no longer change or a stopping criterion is met. For land classification, K-means clustering can group pixels in an image based on spectral properties, such as their reflectance values in different bands. It can identify different land cover types in an image by grouping similar pixels, such as water, vegetation, and urban areas.

We used this method on the surface reflectance values to classify the land cover into four groups, which we then associated with open water, mangrove vegetation, viable land, and bare soil (mud flat). The viable land classification refers to pixels containing either low-density vegetation or bare soil fit for colonization by mangroves. After masking out the open water and bare soil covers, the remaining mangrove vegetation and viable land covers were compared over the years to track the patterns in mangrove cover change and are considered in our supervised analysis. While K-means clustering is a quick method of classifying land cover, we found that it was not sufficiently accurate for our classifications, and it produced inconsistent results within and across observations. As such, we instead use a supervised method for our analysis, as outlined in the next section.

Figure 3. Ground truthing points and classifications from Caroni Swamp, Trinidad and Tobago.

Supervised Learning

Supervised learning is a machine learning paradigm for classifying objects using a set of input objects such as a vector of variables and their desired or human-labeled ("supervised") outputs to train a model. This model can then be used to classify or predict the output of other similar input objects. In a remote sensing context, this set of input objects or training data may look like geolocated points or polygons containing pixels labeled as a certain land cover type or classification. The spectral values of the pixel(s) contained at the point or polygon are then associated with a given category. This is particularly useful here as we can control the classification scheme and make use of ground truthing to validate our models. We used supervised learning to classify the pixels of our satellite imagery into different land type categories, letting us distinguish and track different land cover types systematically. While unsupervised classification methods such as K-means clustering can also be used for land classification on single observations, they lack the higher accuracy and re-usability of supervised methods, which lets us reuse the same trained model on unseen data, giving us a tool to classify land on newly acquired satellite images continuously.

For this study, we use ground-truthing data from the mangroves found in Caroni Swamp, Trinidad and Tobago. The data was collected during a two-day field outing where the locations of different land cover classes were recorded using a Garmin GPSMAP 78sc device. The data comprises 98 data points across the forest (as seen in Figure 3), and is made of the following classes: open water, mangroves, mudflat, intertidal zone, urban, and crops/other vegetation. The data is split in a 70-30 ratio, with 70 percent of the labels randomly selected to be part of the training set and the remaining 30 for our model's testing validation set. In addition to the training set from the Caroni Swamp field cam-

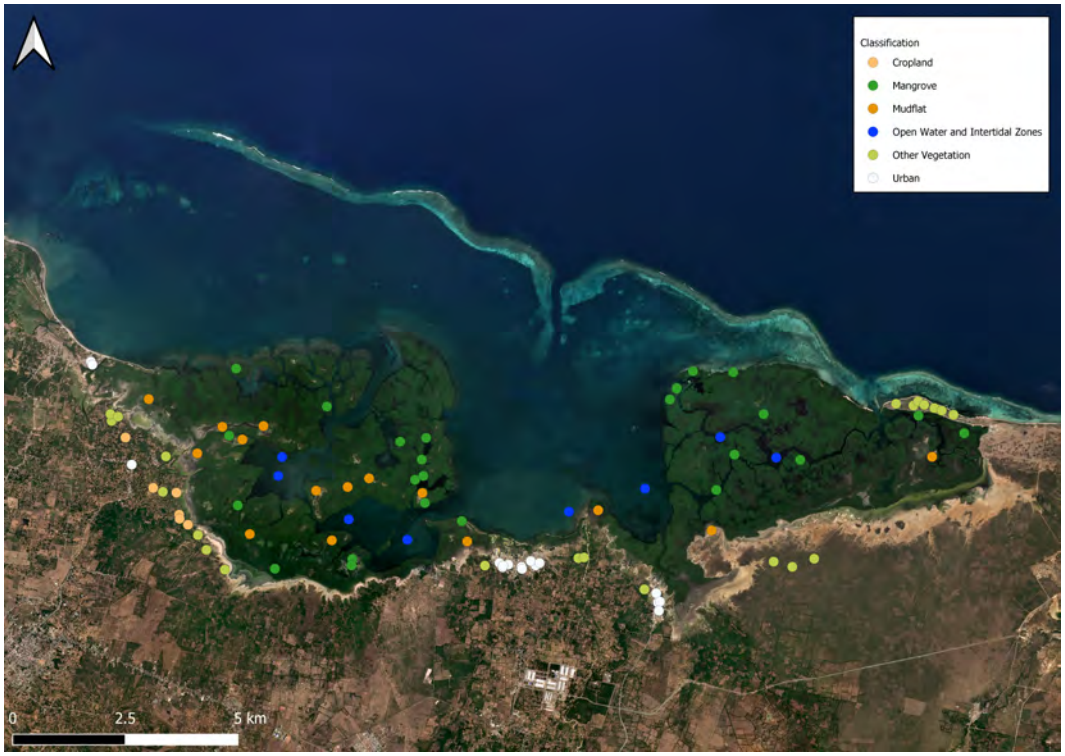

Figure 4. Additional model training points from Caracol Bay, Haiti

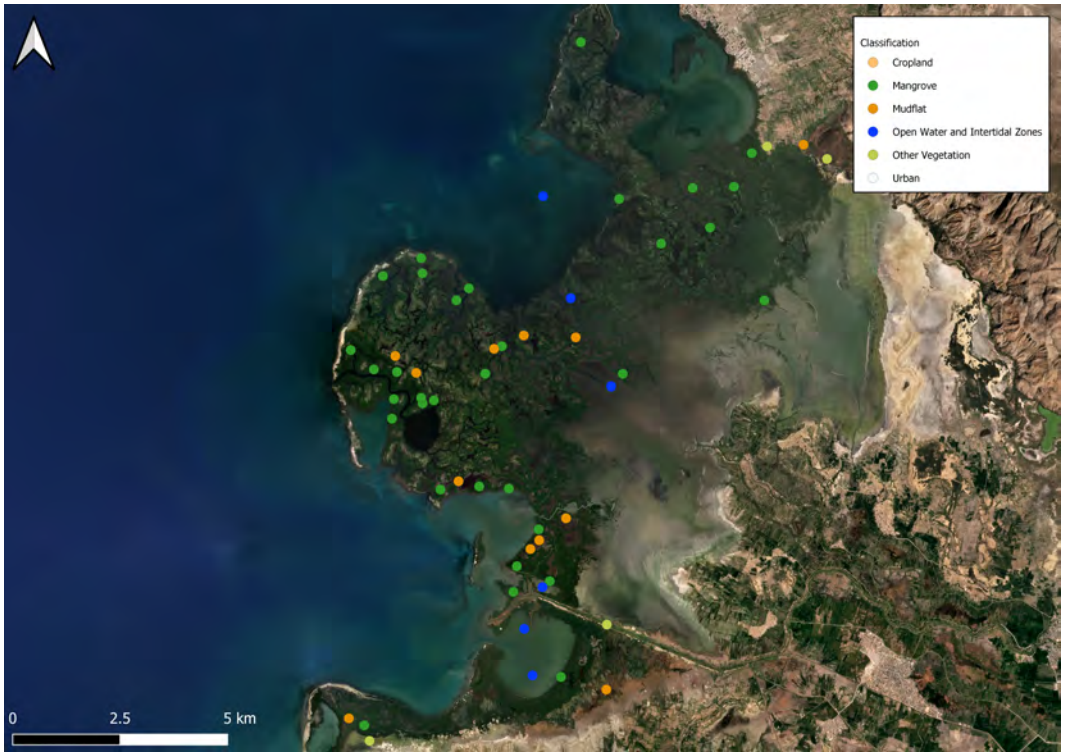

Figure 5. Additional model training points from Grand-Pierre Bay, Haiti

paign, training data points from other mangrove sites in Haiti, namely in Grand-Pierre Bay (Fig. 5) and Caracol Bay (Fig. 4) were also used. These points and their labels were identified using an initial unsupervised classification and confirmed using visual imagery of the sites. As such, while our training set was taken both from this remote identification and ground truths in Caroni Swamp, the validation is exclusively composed of ground truth data points in Caroni Swamp. Using a model trained with this data across Caribbean sites is appropriate here as the tracked ecosystems and landforms are similar, with the same mangrove tree species and land cover types being found across the studied sites.

The algorithm used for our land classification is the Histogram-based Gradient Boosting Classifier (referred to as HGB hereafter) provided in the scikit-learn Python library. HGB is an implementation of the Light Gradient Boosting Machine (LightGBM) framework (Ke et al., 2017) , a widely-used machine learning solution using tree-based learning algorithms and favored for its' fast training speed, low memory usage, and accuracy. LightGBM (and the HGB implementation) was chosen over other machine learning of for its' native support for missing values (NaNs) which would undermine our workflow, as NaN's arise from clouds and any open water pixels that are removed from our images. We use HGB to classify land cover based on the pixels' reflectance values in different bands. The identified mangrove pixels are then masked, isolated, and used in our analysis with vegetation indices to quantify the mangrove forest cover and extent changes as laid out in the following workflow.

Model Validation

Because the classifications made by the model are estimations, we use bootstrapping to conduct its validation. Bootstrapping is a resampling technique where we create multiple new datasets by randomly sampling subsets of the original dataset with replacement. By taking samples from our original dataset and training and evaluating the model multiple times, we can better assess the model's performance variability and robustness.

Results from validation of the trained model on randomly sampled ground-truthed points in Caroni Swamp, Trinidad and Tobago, show robust model performance. This is conducted by resampling, classifying and testing randomly sampled points from the validation set in a bootstrap process, with the data being resampled 800 times. Testing a sample point involves checking whether the classification from the model matches the observed classification from ground-truthing.

To assess the model's performance, we look at the distribution of the mean classification accuracies for each resampling step during the bootstrap process within a 95 percent confidence interval. With this process, we find with model accuracies falling within a 91.4 and 95.9 percent range (Fig. 6). While this shows high general model accuracy, we are also interested in class-based accuracies. The confusion matrix pictured in Fig. 7 A. shows the prediction accuracies for each class in the main diagonal, while the off diagonals show what each class is misclassified as and the ratio of misclassifications. We see a range between 84 and 96 percent for the predicted classes, with the lowest being crops and the highest being mangroves. While the percentage of misclassified crop pixels seems significant - with 3.9% misclassified as urban, 4.3% as mangroves and 8.1% as open water - the total number of misclassified pixels during the bootstrapping process (as seen in Fig. 7B. with the unnormalized matrix) are dwarved by the total number of correctly classified urban, mangroves and open water pixels. As we are principally interested in the cover of mangroves and unvegetated areas of the forest, such as mudflats, we have concluded the model to be robust and appropriate enough for the sake of this analysis.

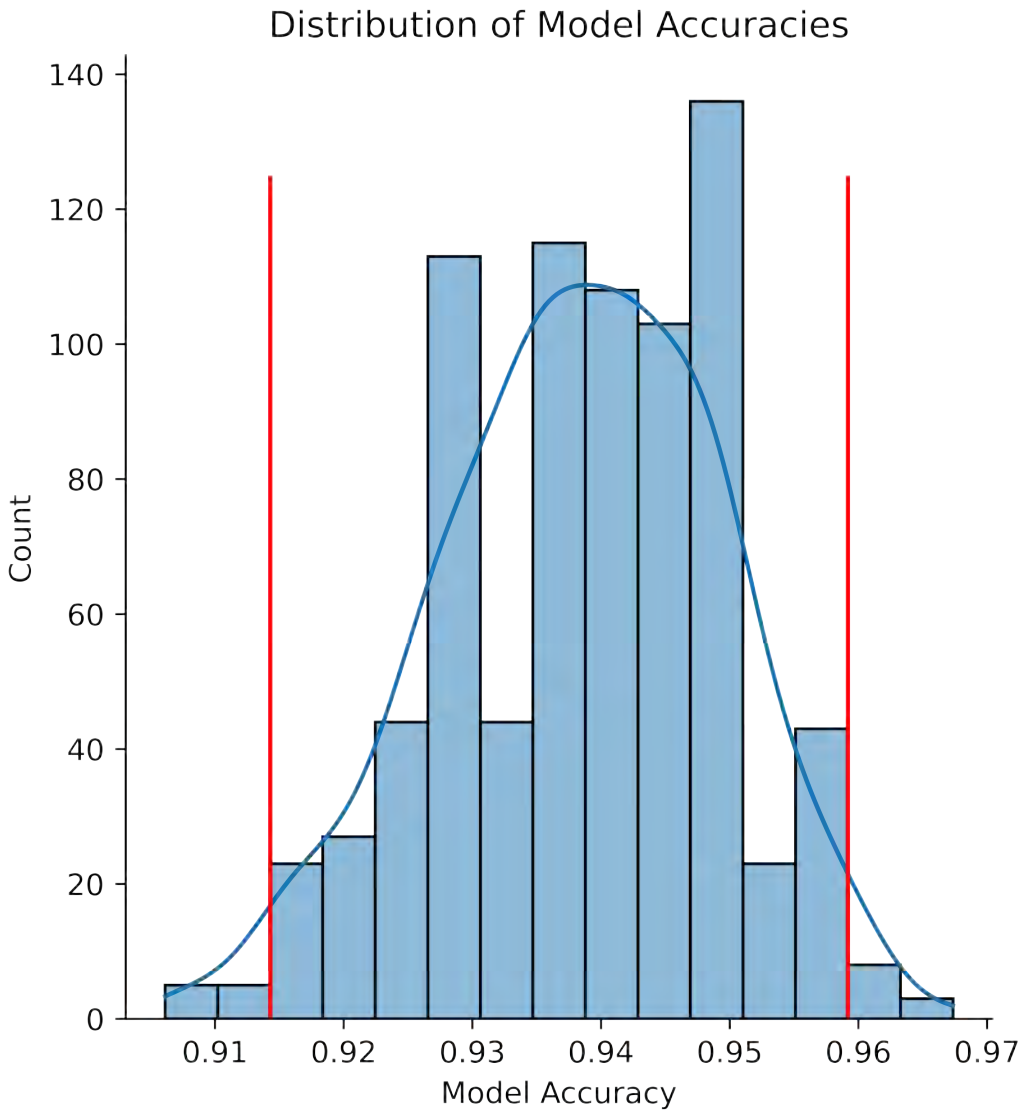

Figure 6. Distribution of Model Accuracies from Bootstrapped Validation Runs.

3.3 Workflow

Our workflow started with acquiring and preprocessing satellite images for which the land cover was classified. We retained the mangrove and mudflat classes for our analysis of the classified land cover types. These classes and the NDVI band in our imagery were used to create products such as time series, metrics, and maps for our analysis. The different components of this workflow (pictured in Fig. 8) and their interactions are outlined in the following subsections.

Preprocessing Images

Images obtained from Planet's archive are screened based on cloud cover, with observations presenting less than 10 percent of cloud cover being retained for analysis. This leaves us with 45 images between 2010 and 2020. Unfortunately, no images were found to be suitable in 2017, as well as the 2011, 2019, and 2020 Wet seasons. While these gaps

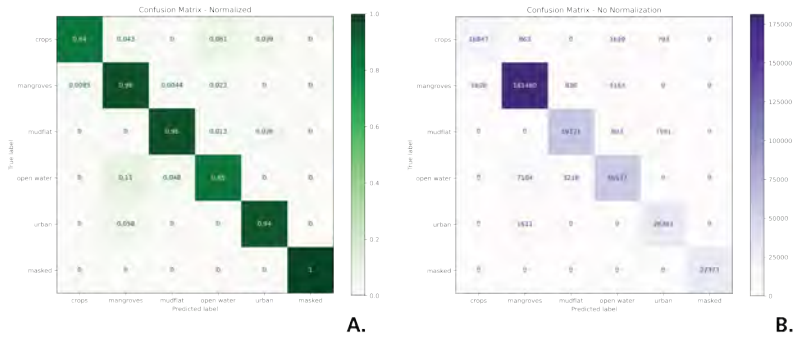

Figure 7. Confusion Matrix of Predicted vs. True Labels of the classification model on Caroni Swamp ground truth points. A. Normalized confusion matrix. B. Unnormalized confusion matrix.

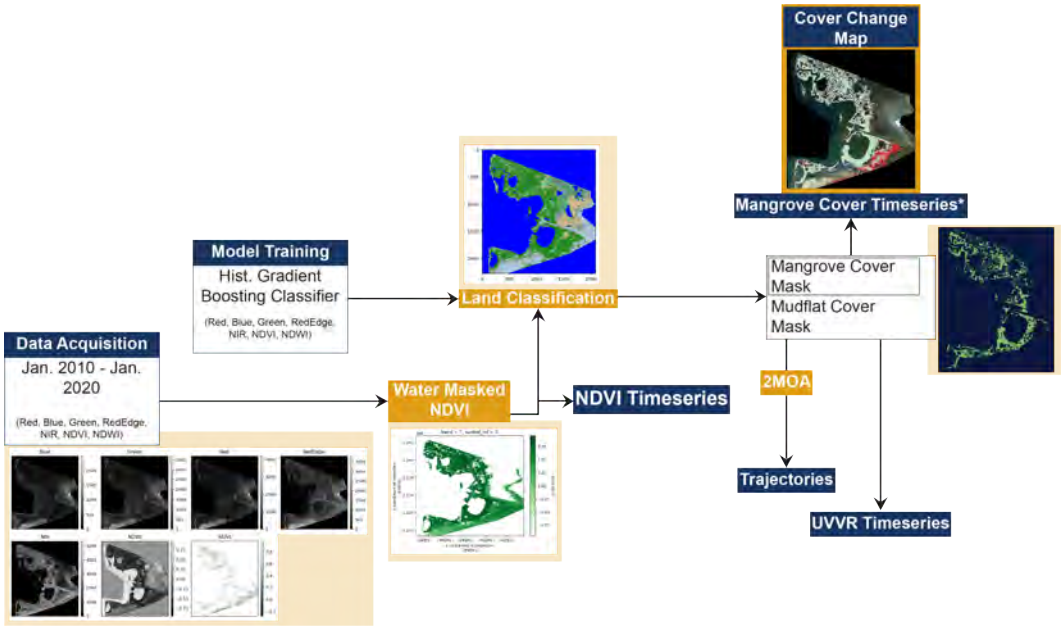

Figure 8. Methods and Tools Workflow

in the data may mean losing some of the finer details of mangrove health progression, we can still make out the overall trends in the 2010 to 2020 period.

Before they are used for either model training or classification of images, the satellite images are preprocessed by masking the open water and urban areas using the NDVI and NDWI indices (defined below). This masking relies on thresholds in these two indices, with NDWI larger than or equal to 0.2 indicating open water pixels and NDVI lower than or equal to 0.2 indicating urban/non-vegetated pixels. Masking open-water and urban areas significantly reduces the complexity of these covers for the model, making it more accurate at predicting these categories.

Model Training and Selection

Following preprocessing, reflectance values across bands are sampled at the locations of our training and validation data points. The hyperparameters of our model were tuned using a grid search, and particular attention was given to the band weights. Be-

cause bands and layers such as RedEdge, NIR, and NDVI are good at detecting and distinguishing vegetation from other cover types (Gandhi et al., 2015), as well as stress within vegetation (Boiarskii & Hasegawa, 2019), we give them a higher class weight in our model. The final parameters used can be found in the Appendix.

Land Classification and Postprocessing

Once the model trained and selected, we used it to classify the 45 observations from Grand-Pierre Bay. From the classified images (featuring open water, mangroves, mudflat, intertidal zone, urban, and crops/other vegetation categories), we created new maps featuring mangrove vegetation and unvegetated regions (by combining mudflats and intertidal zones), leaving us with maps containing only the perceived extents of the mangrove forest by excluding urban, open water, crops, and other vegetation categories. These new maps were then used to compute the metrics defined below on the vegetated and unvegetated sections of the forest.

3.4 Metrics

Gross Cover Change

The gross cover change of mangroves for a given site is the first metric we use to track physical changes in the wetland. While it does not tell us anything about forest density and spatial distribution of vegetation, it is an easy-to-calculate metric for a high-level understanding of how the mangrove evolves. The gross cover of a single observation is calculated by counting the number of pixels classified as mangroves and multiplying that number by the resolution of a single pixel, as provided by the specifications of the utilized satellite instrument. The Gross Cover Change is then the difference in gross mangrove cover between the two observation dates.

Unvegetated to Vegetated Ratio - UVVR

The Unvegetated to Vegetated Ratio is an index that helps establish vegetation cover status and track wetland changes (Couvillion et al., 2021). It does so by taking the ratio of unvegetated pixels (such as mud flats) to the vegetated pixels (like mangroves in our case). The closer to zero our UVVR, the more vegetation there is in our site and the more dense this forest is. At values of UVVR above 1.0, the forest has significant regions of unvegetated, exposed soil. As such, increases in UVVR over time indicate loss of mangrove forest, which could be due to natural disasters, changes in environmental conditions, or deforestation due to human activity. Conversely, decreases in UVVR denote afforestation. We implement this simple relation as follows for each observation:

$$UVVR = \frac{\#mangrove}{\#mudflats + \#intertidalzone}$$

where # is the "number of pixels of."

4 Results and Discussion

Our analysis of forest health dynamics in Grand-Pierre Bay then revolves around the spatio-temporal changes in NDVI values within the mangrove vegetation pixels, as identified by our supervised classification algorithm and their distribution. The NDVI observations are sorted and aggregated per seasons and years. Haiti presents 2 distinct seasons: wet and dry, with the wet season going from April to October, and the dry season going from November to March.

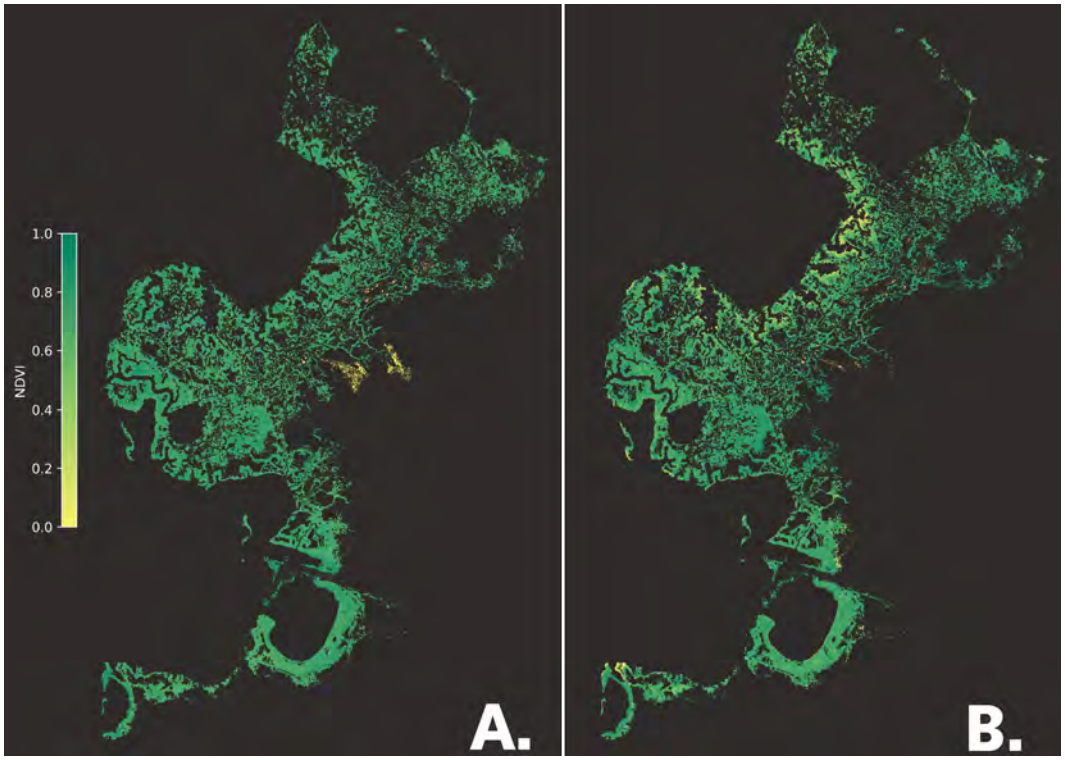

Figure 9. Aggregated mangrove pixels and their NDVI values. A. Mangrove cover and NDVI in 2010. B. Mangrove cover and NDVI in 2020.

4.1 Change in NDVI

To capture and analyze the spatial changes in mangrove health, we use and compare the aggregated pixels classified as mangroves and their NDVI values in 2010 and 2020 (Fig. 9). Displayed in those images are the pixels classified as mangroves for each year, as well as the NDVI values within them. The yellow colors stand out as locations where forest health is suffering, and the difference between 2010 (left) and 2020 (right) can most strikingly be seen along the seaward edge, with the 2020 image showing deteriorating forest health along its boundary.

By formally taking the difference in NDVI values between the aggregated data for the years 2010 and 2020 (dNDVI), we can identify and map pixels in the 2020 cover with decreases and increases in NDVI, with negative dNDVI values signifying reduced vegetation health or death, and positive values signifying increased health or growth. As seen in Figure 10, the forest includes regions of decline and growth. This pattern here is displayed in terms of percentage change for a given pixel. While the change can have larger magnitudes than 100 percent, we limit the scale to +100 and -100 for a better visualization of the spatial distribution of change; with NDVI values of vegetation generally ranging between 0.2 and 1, the death of mangroves is seen as sharp declines from the vegetation range into values close to zero or negatives as cover transitions to bare soil/mud and open water. Conversely, new growth and establishments display sharp increases in NDVI values into the vegetation range. Because NDVI varies between -1 and 1, these sharp changes frequently create relative changes larger than 100 percent (i.e., a pixel with a positive value in 2010 could be negative in 2020). Displaying the full range of percent change then puts a highlight on the deaths and new growths of mangroves,

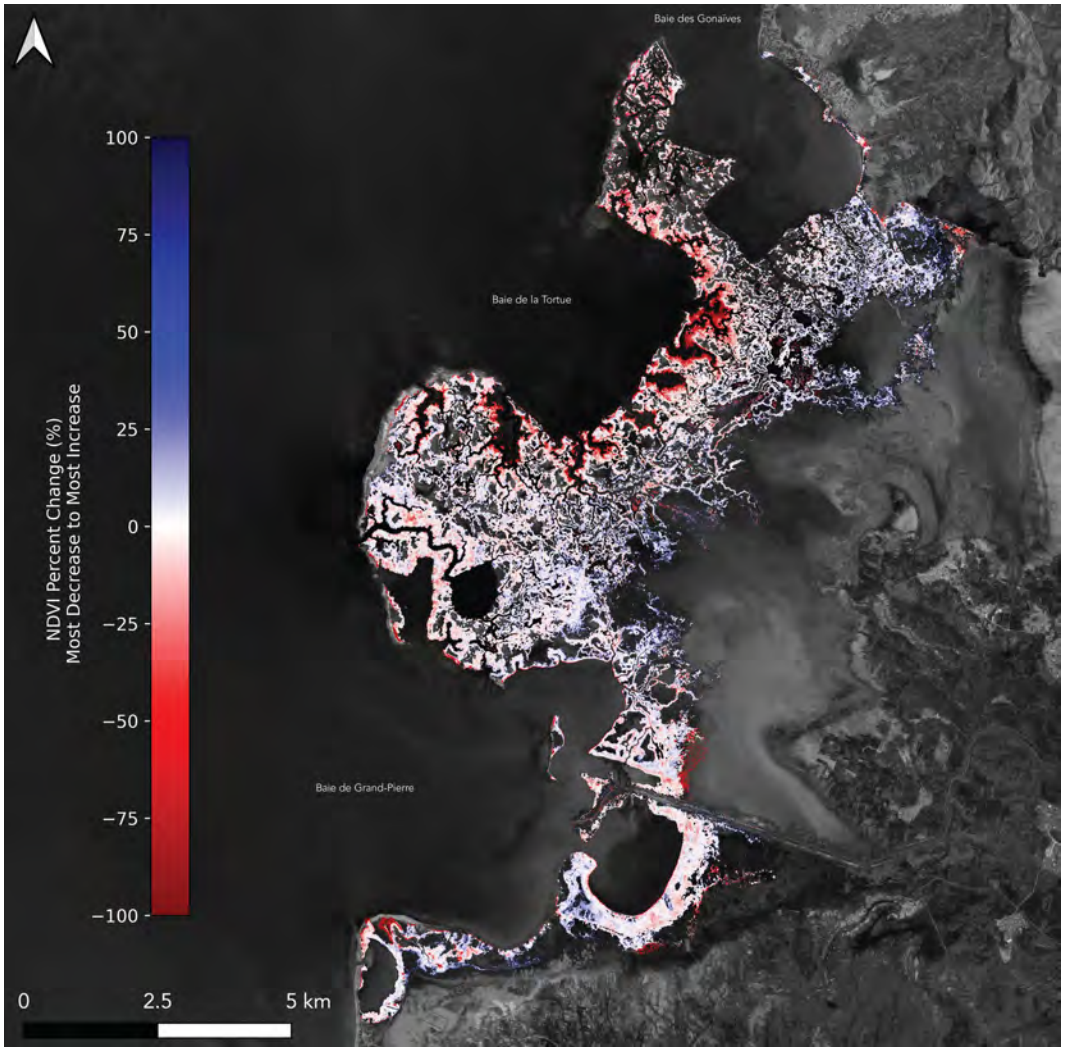

Figure 10. Change in NDVI within mangrove cover between 2020 and 2010.

while losing the finer details of decreasing and increasing health in perpetuating mangroves.

The declines are concentrated in the sea-facing areas (seaward), particularly in the central embayment of our site in Baie de la Tortue, while pockets of growth appear in the lagoon and land-facing areas (landward). This spatial distribution indicates a landward retreat of the forest. With areas showing declines in NDVI of 100 percent and more, indicating the possible death of vegetation, the forest is experiencing diebacks on its coastal front, while having renewed health and growth next to the lagoon.

4.2 Mangrove Cover Change

Similarly, we use the 2010 and 2020 aggregated mangrove covers (pixels classified as mangrove) to capture the change in mangrove cover. Through comparison with the 2010 land cover classification, we identify pixels in the 2020 land cover classification in which mangrove was lost (the pixel was classified as mangrove in 2010, but not in 2020), mangrove was gained (was not mangrove in 2010, but was in 2020), and remained the same (was classified as mangrove in both 2010 and 2020). This mangrove cover change

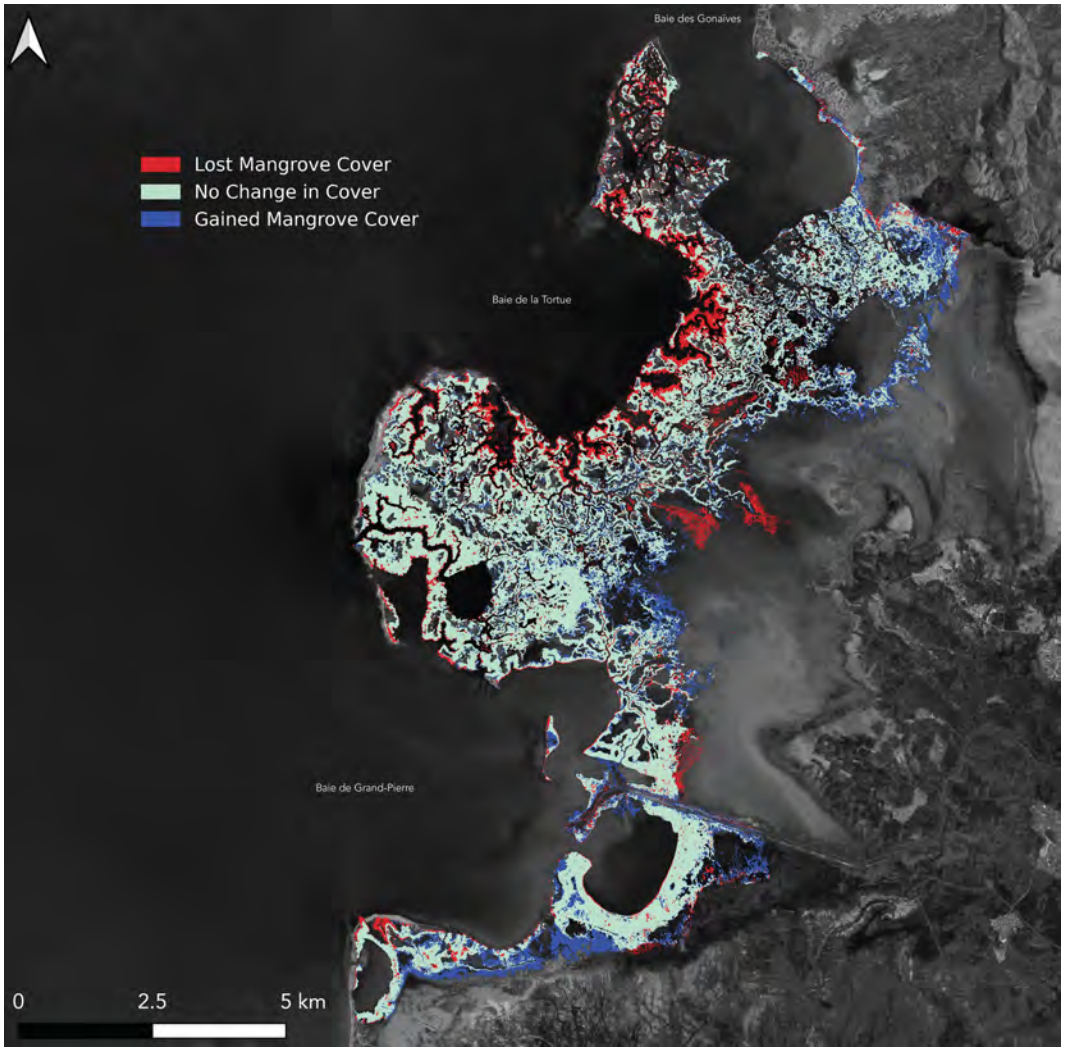

Figure 11. Change in mangrove cover between 2010 and 2020.

map (Fig. 11) shows areas of mangrove retreat and new growth. The spatial change in NDVI showed strong health declines seaward, and increases landward. This is corroborated by the change in mangrove cover, with systematic retreat seen seaward, particularly around Baie de la Tortue, while new growth is seen across the landward boundary of the forest.

The changes in mangrove health across the forest were stark enough to trigger diebacks and also change the forest's cover composition. Using the change in detected mangrove cover, we observe reduced mangrove cover mainly in the Baie de la Tortue between 2010 and 2020. Following the gross mangrove cover and UVVR progression and their year-to-year percent change in Table 1, we see a sharp decline in mangrove cover and UVVR in 2013, followed by a timid and varied recovery of mangrove cover, most likely driven by new growth landward of the forest. While there was a strong initial recovery of cover and UVVR in 2014, this recovery stalls in 2017, and the forest cover and ratio of vegetation to unvegetated did not recover to pre-2013 levels, implying that while the forest showed some resilience, it displays a net loss of cover, and the recovery and landward migration of cover did not keep up with the continued loss on the coastline.

Table 1. Mangrove Cover and UVVR Evolution

Year	Mangrove Cover (km^2)	Percent Change	UVVR	Percent Change
2010	198.688	–	1.065	–
2011	200.989	1.158	1.091	2.513
2012	211.319	5.139	1.192	9.216
2013	187.708	-11.173	0.985	-17.360
2014	195.841	4.333	1.060	7.643
2015	198.585	1.401	1.058	-0.186
2016	201.019	1.226	1.098	3.729
2017	195.354	-2.818	1.013	-7.731
2018	198.919	1.825	1.061	4.760
2019	190.856	-4.054	0.947	-10.784
2020	196.018	2.705	0.983	3.802

With this new growth landward within the lagoon and intertidal zones, the Grand-Pierre Bay mangrove forest is effectively migrating landward and retreating from the coastline. This process is unfortunately unsustainable, as it appears that even over the 10-year observation period, the landward progression of the mangrove was insufficient to offset the loss of forest on its seaward edge. Additionally, there is the question of space, as not all of the intertidal zone may be suitable for new establishments, and that space is limited. This has implications for the coastal defense properties of this mangrove forest in the future that will need to be further studied to better assess its role in the coastal protection of this region.

4.3 Spatio-Temporal Change in the Forest

This pattern of decline and growth in the forest was not a constant spatial or temporal process. In Fig. 12 , stacked ridge plots show the seasonal variation of NDVI values found in the forest across the observation period. NDVI values from all observations are aggregated per season, wet and dry, across the decade of observations, with each ridge displaying the distribution of values for each season. A look at seasonal NDVI distributions within the mangrove forest, while having alternating trends pre-2013, shows a consistent decrease in mangrove health after the 2013 dry season. This decline slows down in 2016, with distributions having smaller left tails and lower upper bounds 2018 forward. This move and change in the distributions may indicate a reorganization in the forest structure. This restructuring of the forest would hint at an underlying environmental process driving this redistribution of cover.

Two possible candidates are sea-level rise and changes in climate and precipitation. Between 2013 and 2015, Haiti suffered through the unprecedented Pan-Caribbean drought, which heavily impacted precipitations, freshwater outflows, and precipitation-evapotranspiration balance in the region (Herrera et al., 2018). Precipitation estimates from CHIRPS show a sharp decline in wet season precipitations in the Artibonite region. Figure 14, which displays the distribution of precipitations in wet and dry seasons from 2000 to 2021 water years, features a strong decline between 2013 and 2016, with lower means and heavy precipitation in both the wet and dry seasons, confirming lower precipitation and freshwater inputs in the forest.

Coincidentally, tide gauge data around the island of Haiti showcase rises in local sea level between 2010 and 2015, followed by a decrease between 2015 and 2017 (Fig. 15). While the lack of long-term, continuous tidal data in the region makes it hard to characterize regional sea-level rise, this local variation in sea-level across the island indicates possible sea and wave action stressors on the coastline of the mangrove forest.

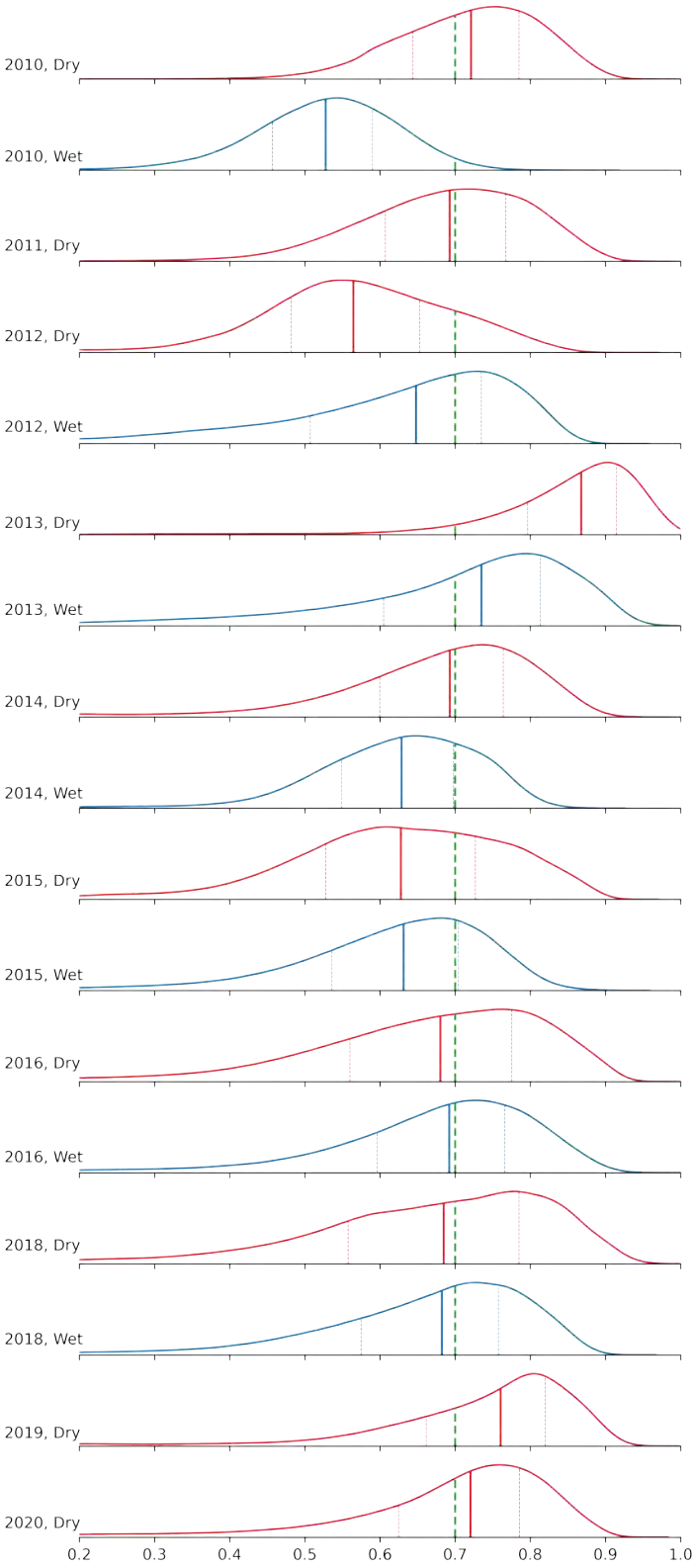

Figure 12. Seasonal Distribution of NDVI values within mangrove cover in Grand-Pierre Bay. The green dotted line represents the NDVI threshold for healthy vegetation (NDVI = 0.7).

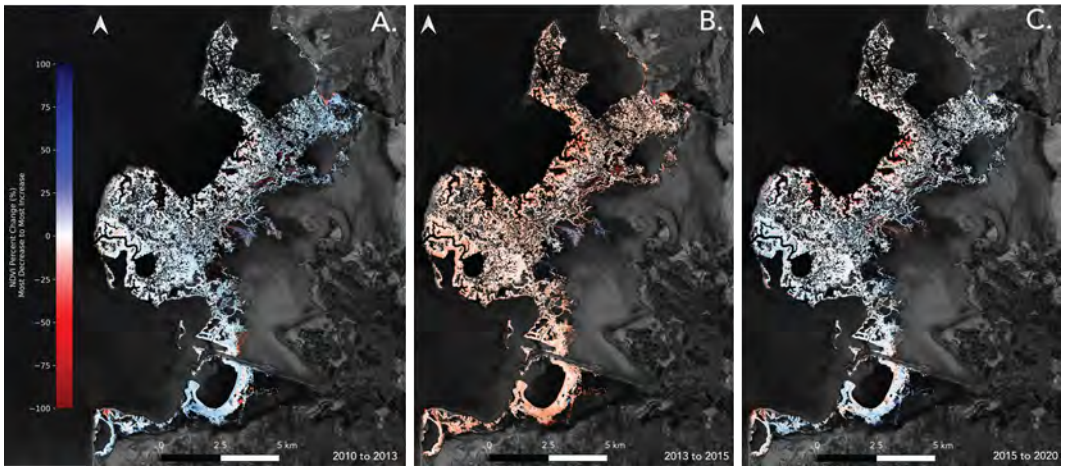

Figure 13. Progression of NDVI changes during the 2010 decade. A. Features the pre-drought changes (2010-2013). B. Features change during the drought period (2013-2015). C. Features post-drought changes (2015-2020).

This change in structure can be seen by looking at the time progression of spatial change in forest health. (Fig. 13) shows the spatial change in NDVI between the following three periods: pre-drought 2010-2013 (Fig. 13A.), drought 2013-2015 (Fig. 13B.), and post-drought 2015-2020 (Fig. 13C.). While some light decline can be seen in the Baie de la Tortue, the forest sees increases in NDVI in most locations. The 2013-2015 drought period saw a uniform decline in the forest, most accentuated in coastal-facing areas. The post-drought recovery of the forest is, however, not uniform, with the decline continuing in the coastal facing regions and light increases in NDVI occurring in the landward regions. Looking at these three periods, we observe that the Pan-Caribbean drought coincides with an acceleration of the seaward loss of mangroves.

We hypothesize that the reduced freshwater inputs from the drought likely raised the salinity levels in the forest, leaving mangroves more vulnerable to sea action and other environmental stressors. A review on the environmental drivers of mangrove establishment and early development by (Krauss et al., 2008) frames temperature, light, flooding, salinity, and nutrients as the major ecophysiological health factors for this critical life stage of mangroves. While we were not able to acquire observations of local temperature or light changes, it is safe to say that the combined effects of drought and rising local sea levels would disrupt flooding regimes, freshwater inputs, and nutrient inputs from rivers. These disruptions would potentially raise salinity levels in the forest, decrease nutrient inputs, and expose the coastal front of the forest. The spatial variability in mangrove health and cover change is then most likely the result of the combined actions of regional sea-level rise on weakened mangrove trees in low-lying areas farthest from river outflows, which were likely most impacted by high salinity during the drought, leading to diebacks, and more difficult reestablishment in the same areas.

5 Conclusions

A sharp decline in mangrove cover and health was observed during the 2013-2016 Haitian drought, followed by a spatially heterogeneous recovery, with most of it occurring on the landward area of the forest and continued retreat happening along its seaward edge, particularly along the shore of Baie de la Tortue (Fig. 1). This indicates resilience to environmental stressors in the forest, but not an equal one; as the forest re-

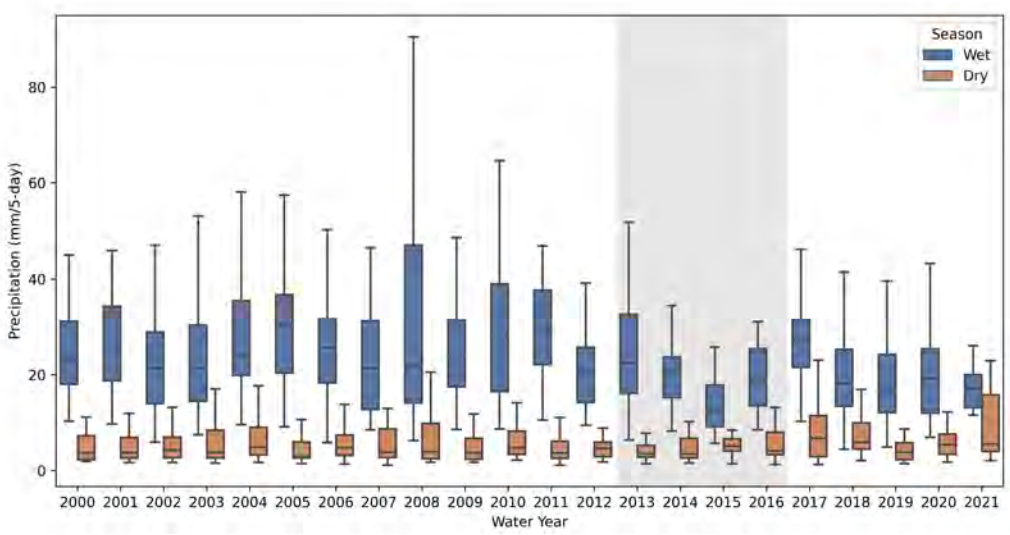

Figure 14. Estimated Precipitation Distributions in the Artibonite Region. Estimations are generated by ClimateEngine.org through the CHIRPS dataset (2000-2020).

covers from lowered freshwater inputs and local rises in sea-level, the forest migrates landward. This landward migration is unsustainable, as it may not be able to occur fast enough to keep up with the increased frequency and severity of climate change induced environmental stressors, and as not all of the available space landward is suitable for mangrove establishment.

To ensure the continuation of the protection benefits of this mangrove forest, targeted conservation and restoration efforts may be needed on forest's most vulnerable regions on the coastline, while supporting the further establishment of mangroves landward. Based on these new understandings of how mangrove forest may evolve under climate forcing, future work may include hydrodynamic studies to quantify the change in protection services offered by this landform. Only with an integrated consideration of how the ecology and the climate forcing evolve can we achieve a resilient future that makes most effective use of these natural protective features.

Open Research Section

Rainfall estimates can be accessed from the Climate Hazard Center database at UC Santa Barbara via the ClimateSERV online toolkit: `https://climateserv.servirglobal.net`. To obtain the data, follow the "Getting Started" link, then upload a zipped shapefile of the Artibonite River Watershed as an Area of Interest (AOI). This file is available in the project's GitHub repository under `datasets/Shapefiles/Artibonite_AOI.zip`. Next, select "Observation" as the Data Type, choose "UCSB CHIRPS Rainfall" as the Data Source, set the Calculation to "Average," and specify a date range from 01/01/2000 to 12/31/2020. Ensure that you "Add Query" and then "Submit Query." After processing, the dataset will be available for download as a .csv file.

Alternatively, the raw precipitation raster files are accessible in the CHIRPS dataset directory at `https://data.chc.ucsb.edu/products/CHIRPS-2.0`. Monthly rainfall estimates for the Caribbean are available in the `camer-carib_monthly` directory, while global daily estimates can be found in the `global_daily` directory. Using the AOI, mean daily precipitation can be derived for the same time period.

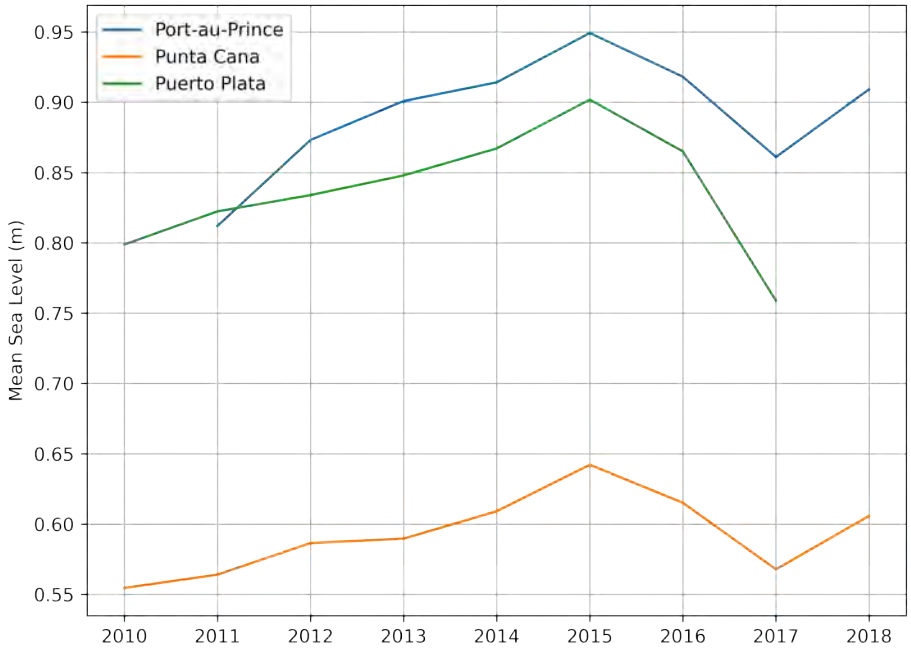

Figure 15. Yearly mean sea levels from tide gauge data in Haiti and the Dominican Republic.

Tidal gauge data in Port-au-Prince, Punta Cana and Puerto Plata are hosted by the University of Hawaii Sea Level Center and can be accessed through GESLA (Global Extreme Sea Level Analysis) (Haigh et al., 2021), (Woodworth et al., 2016), (Caldwell et al., 2015): `https://gesla787883612.wordpress.com/downloads/`

All processed satellite imagery, data products and supporting data can be accessed from this project's GitHub page: `https://github.com/aesgeorges/MangroveCaribRS`

Acknowledgments

I would like to extend my gratitude to Hearts to Humanity (H2H8), whose generous support enabled the successful carryout of this work. I am thankful for the support of my colleagues and faculties in the Environmental Fluid Mechanics and Hydrology group at UC Berkeley and their constructive feedback. Likewise, inputs from Jean Wiener of FoProBim was invaluable to the shaping of the scope of this project. Finally, I'd like to express my deepest gratitude to my parents, my sister, friends from Haiti and elsewhere, and Claire, who saw me at every step of this project.

References

Assessing the Potential Impact of Climate Change on Rice Yield in the Artibonite Valley of Haiti Using the CSM-CERES-Rice Model. (n.d.). Retrieved 2024-07-01, from `https://doi.org/10.13031/trans.13868`

Boiarskii, B., & Hasegawa, H. (2019, November). Comparison of NDVI and NDRE Indices to Detect Differences in Vegetation and Chlorophyll Content. *JOURNAL OF MECHANICS OF CONTINUA AND MATHEMATICAL SCI-*

ENCES, *spl1*. doi: 10.26782/jmcms.spl.4/2019.11.00003

Caldwell, P., Merrifield, M. A., & Thompson, P. R. (2015). *Sea level measured by tide gauges from global oceans — the Joint Archive for Sea Level holdings (NCEI Accession 0019568), Version 5.5.* NOAA National Centers for Environmental Information. Retrieved 2024-08-19, from http://doi.org/10.7289/V5V40S7W (Last Modified: 2024-07-29) doi: http://doi.org/10.7289/V5V40S7W

Chen, Q., Li, Y., Kelly, D. M., Zhang, K., Zachry, B., & Rhome, J. (2021, October). Improved modeling of the role of mangroves in storm surge attenuation. *Estuarine, Coastal and Shelf Science*, *260*, 107515. Retrieved 2023-11-20, from https://www.sciencedirect.com/science/article/pii/S0272771421003668 doi: 10.1016/j.ecss.2021.107515

Couvillion, B., Ganju, N. K., & Defne, Z. (2021). *An Unvegetated to Vegetated Ratio (UVVR) for coastal wetlands of the Conterminous United States (2014-2018).* U.S. Geological Survey. Retrieved 2024-08-05, from https://www.sciencebase.gov/catalog/item/5fa18656d34e198cb793cba5 doi: 10.5066/P97DQXZP

Crase, B., Liedloff, A., Vesk, P., Burgman, M., & Wintle, B. (2013, July). Hydroperiod is the main driver of the spatial pattern of dominance in mangrove communities. *Global Ecology & Biogeography*, *22*. doi: 10.1111/geb.12063

Duncan, C., Owen, H. J. F., Thompson, J. R., Koldewey, H. J., Primavera, J. H., & Pettorelli, N. (2018). Satellite remote sensing to monitor mangrove forest resilience and resistance to sea level rise. *Methods in Ecology and Evolution*, *9*(8), 1837–1852. Retrieved 2022-05-24, from https://onlinelibrary.wiley.com/doi/abs/10.1111/2041-210X.12923 (_eprint: https://onlinelibrary.wiley.com/doi/pdf/10.1111/2041-210X.12923) doi: 10.1111/2041-210X.12923

Funk, C., Peterson, P., Landsfeld, M., Pedreros, D., Verdin, J., Shukla, S., ... Michaelsen, J. (2015, December). The climate hazards infrared precipitation with stations—a new environmental record for monitoring extremes. *Sci Data*, *2*(1), 150066. Retrieved 2024-08-19, from https://www.nature.com/articles/sdata201566 (Publisher: Nature Publishing Group) doi: 10.1038/sdata.2015.66

Gandhi, G. M., Parthiban, S., Thummalu, N., & Christy, A. (2015, January). Ndvi: Vegetation Change Detection Using Remote Sensing and Gis – A Case Study of Vellore District. *Procedia Computer Science*, *57*, 1199–1210. Retrieved 2024-08-05, from https://www.sciencedirect.com/science/article/pii/S1877050915019444 doi: 10.1016/j.procs.2015.07.415

Haigh, I. D., Marcos, M., Talke, S. A., Woodworth, P. L., Hunter, J. R., Hague, B. S., ... Thompson, P. (2021, November). GESLA Version 3: A major update to the global higher-frequency sea-level dataset. Retrieved 2024-08-19, from https://eartharxiv.org/repository/view/2828/ (Publisher: EarthArXiv)

Herrera, D. A., Ault, T. R., Fasullo, J. T., Coats, S. J., Carrillo, C. M., Cook, B. I., & Williams, A. P. (2018). Exacerbation of the 2013–2016 Pan-Caribbean Drought by Anthropogenic Warming. *Geophysical Research Letters*, *45*(19), 10,619–10,626. Retrieved 2024-07-13, from https://onlinelibrary.wiley.com/doi/abs/10.1029/2018GL079408 (_eprint: https://onlinelibrary.wiley.com/doi/pdf/10.1029/2018GL079408) doi: 10.1029/2018GL079408

Ikotun, A. M., Ezugwu, A. E., Abualigah, L., Abuhaija, B., & Heming, J. (2023, April). K-means clustering algorithms: A comprehensive review, variants analysis, and advances in the era of big data. *Information Sciences*, *622*, 178–210. Retrieved 2024-07-02, from https://www.sciencedirect.com/science/article/pii/S0020025522014633 doi: 10.1016/j.ins.2022.11.139

Jean-Baptiste, N., & Jensen, J. R. (2006, December). Measurement of Mangrove Biophysical Characteristics in the Bocozelle Ecosystem in Haiti Using ASTER Multispectral Data. *Geocarto International*, *21*(4), 3–8. Retrieved 2023-11-30, from https://doi.org/10.1080/10106040608542397 (Publisher: Taylor & Francis _eprint: https://doi.org/10.1080/10106040608542397) doi: 10.1080/10106040608542397

Ke, G., Meng, Q., Finley, T., Wang, T., Chen, W., Ma, W., ... Liu, T.-Y. (2017). LightGBM: A Highly Efficient Gradient Boosting Decision Tree. In *Advances in Neural Information Processing Systems* (Vol. 30). Curran Associates, Inc. Retrieved 2024-10-17, from https://papers.nips.cc/paper_files/paper/2017/hash/6449f44a102fde848669bdd9eb6b76fa-Abstract.html

Krauss, K. W., Lovelock, C. E., McKee, K. L., López-Hoffman, L., Ewe, S. M. L., & Sousa, W. P. (2008, August). Environmental drivers in mangrove establishment and early development: A review. *Aquatic Botany*, *89*(2), 105–127. Retrieved 2023-09-26, from https://www.sciencedirect.com/science/article/pii/S0304377008000089 doi: 10.1016/j.aquabot.2007.12.014

Lagomasino, D., Fatoyinbo, T., Castañeda-Moya, E., Cook, B. D., Montesano, P. M., Neigh, C. S. R., ... Morton, D. C. (2021, June). Storm surge and ponding explain mangrove dieback in southwest Florida following Hurricane Irma. *Nat Commun*, *12*(1), 4003. Retrieved 2023-11-06, from https://www.nature.com/articles/s41467-021-24253-y (Number: 1 Publisher: Nature Publishing Group) doi: 10.1038/s41467-021-24253-y

Lovelock, C. E., Feller, I. C., Reef, R., Hickey, S., & Ball, M. C. (2017, May). Mangrove dieback during fluctuating sea levels. *Sci Rep*, *7*(1), 1680. Retrieved 2023-11-06, from https://www.nature.com/articles/s41598-017-01927-6 (Number: 1 Publisher: Nature Publishing Group) doi: 10.1038/s41598-017-01927-6

Maza, M., Adler, K., Ramos, D., Garcia, A. M., & Nepf, H. (2017, November). Velocity and Drag Evolution From the Leading Edge of a Model Mangrove Forest. *Prof. Nepf via Elizabeth Soergel*. Retrieved 2023-11-20, from https://dspace.mit.edu/handle/1721.1/119430 (Accepted: 2018-12-04T19:54:28Z Publisher: American Geophysical Union (AGU))

Montgomery, J. M., Bryan, K. R., Mullarney, J. C., & Horstman, E. M. (2019). Attenuation of Storm Surges by Coastal Mangroves. *Geophysical Research Letters*, *46*(5), 2680–2689. Retrieved 2023-11-20, from https://onlinelibrary.wiley.com/doi/abs/10.1029/2018GL081636 (_eprint: https://onlinelibrary.wiley.com/doi/pdf/10.1029/2018GL081636) doi: 10.1029/2018GL081636

Murakami, H., Delworth, T. L., Cooke, W. F., Zhao, M., Xiang, B., & Hsu, P.-C. (2020, May). Detected climatic change in global distribution of tropical cyclones. *Proceedings of the National Academy of Sciences*, *117*(20), 10706–10714. Retrieved 2022-05-13, from https://www.pnas.org/doi/10.1073/pnas.1922500117 (Publisher: Proceedings of the National Academy of Sciences) doi: 10.1073/pnas.1922500117

Pokhriyal, N., Zambrano, O., Linares, J., & Hernández, H. (n.d.). Estimating and Forecasting Income Poverty and Inequality in Haiti.

Sadeh, Y., Zhu, X., Dunkerley, D., Walker, J. P., Zhang, Y., Rozenstein, O., ... Chenu, K. (2021, April). Fusion of Sentinel-2 and PlanetScope time-series data into daily 3 m surface reflectance and wheat LAI monitoring. *International Journal of Applied Earth Observation and Geoinformation*, *96*, 102260. Retrieved 2023-10-03, from https://www.sciencedirect.com/science/article/pii/S030324342030903X doi: 10.1016/j.jag.2020.102260

Salas-Rabaza, J. A., Reyes-García, C., Méndez-Alonzo, R., Us-Santamaría, R., Flores-Mena, S., & Andrade, J. L. (2023, December). Hydroperiod modulates early growth and biomass partitioning in Rhizophora man-

gle L. *Aquatic Botany*, 103747. Retrieved 2023-12-25, from https://www.sciencedirect.com/science/article/pii/S0304377023001328 doi: 10.1016/j.aquabot.2023.103747

Woodworth, P. L., Hunter, J. R., Marcos, M., Caldwell, P., Menéndez, M., & Haigh, I. (2016). Towards a global higher-frequency sea level dataset. *Geoscience Data Journal*, *3*(2), 50–59. Retrieved 2024-08-19, from https://onlinelibrary.wiley.com/doi/abs/10.1002/gdj3.42 (_eprint: https://onlinelibrary.wiley.com/doi/pdf/10.1002/gdj3.42) doi: 10.1002/gdj3.42

Zhang, K., Liu, H., Li, Y., Xu, H., Shen, J., Rhome, J., & Smith, T. J. (2012, May). The role of mangroves in attenuating storm surges. *Estuarine, Coastal and Shelf Science*, *102-103*, 11–23. Retrieved 2022-05-24, from https://www.sciencedirect.com/science/article/pii/S0272771412000674 doi: 10.1016/j.ecss.2012.02.021

Remote Sensing Study of Mangrove Forest Health and Resilience in the Grand-Pierre Bay, Artibonite, Haiti

Alexandre E. S. Georges[1*], Mark T. Stacey[1], Deanesh Ramsewak[2]

[1]University of California, Berkeley
[2]Centre for Maritime and Ocean Studies, The University of Trinidad and Tobago

Key Points:

- The 2013 Pan-Caribbean drought weakened the Grand-Pierre Bay mangrove forest in Haiti. Recovery was uneven, with continued coastal retreat.
- Tide gauge data in Haiti showed local sea-level rises partly coinciding with the Pan-Caribbean drought. This combination of environmental factors likely stressed the mangrove forest, contributing to the observed pattern of coastal retreat and landward migration.
- The forest's landward migration is unsustainable as the available landward space may not support continued mangrove establishment, raising concerns about the long-term resilience of the forest.

[*]H2H8

Corresponding author: Alexandre Georges, alexandre_georges@berkeley.edu

Abstract

As climate change increases the vulnerability of Small Island Developing States' marginalized coastal communities and ecosystems, it is necessary to evaluate the health and resilience of their natural landforms and infrastructure inventories. For example, mangroves could be a central component of coastal adaptation strategies for these sites due to their storm surge attenuating properties. One such forest is located in Haiti in the Grand-Pierre Bay, south of Gonaives and at the mouth of the Artibonite Valley, a region important for its agriculture. A remote sensing study of the Grand-Pierre Bay mangroves was conducted using imagery from PlanetLabs, machine learning tools, and vegetation health indices to identify and track mangrove cover, health, and spatio-temporal changes between 2010 and 2020. Detected changes in cover and NDVI (Normalized Difference Vegetation Index) values display a retreat of mangrove cover from the sea, with most of the retreat and health loss occurring during the 2013-2016 Pan-Caribbean drought, which was also experienced in Haiti. While the forest displays recovery post-drought, health increases and new establishments are concentrated on the landward side of the forest, and continued retreat is occurring on the shoreline, indicating a landward migration of the forest. This migration may, however, not occur fast enough to offset the losses on the coast, and targeted conservation efforts may be required to sustain and enhance the forest's resilience.

Plain Language Summary

As climate change's impact on Small Island Developing States becomes more apparent, evaluating how their natural environments cope is essential. Coastal communities in these states often benefit from natural defenses like mangrove forests for protection against flooding. This study focuses on the Grand-Pierre Bay mangrove forest in Haiti, located south of Gonaives and at the mouth of the Artibonite Valley, a vital agricultural area.

By analyzing satellite images and land cover maps, we tracked changes in the forest's size and health between 2010 and 2020. Results showed the forest was stressed and retreating, with the most loss occurring between 2013 and 2016, coinciding with the Pan-Caribbean drought. While inland areas are recovering, the coastline mangroves continue to decline, indicating landward migration.

We suggest that reduced freshwater input and rising sea levels contributed to this decline. If these current trends continue, this would have serious implications for mangrove resilience and their ability to protect against flooding in this area.

1 Introduction

In the face of escalating climate change impacts worldwide, governments and communities are looking at possible adaptation pathways to mitigate its effects. For Small Island Developing States (SIDS) in the Caribbean, the use of natural landforms such as wetlands in coastal defense infrastructure provides some optimism. Due to increased hurricane activity in the North Atlantic (Murakami et al., 2020), the Caribbean islands are particularly vulnerable to the impacts of climate change on coastlines, with increased flooding due to storm surges being expected as a result. In Haiti, this increased coastal vulnerability disproportionately impacts disadvantaged urban and rural populations and critical economic centers; out of the 10 communes (municipalities) with the largest number of people living in income poverty in 2012 in Haiti, 7 are coastal (Pokhriyal et al., n.d.). Mangrove forests, which are native to the region, may be viable candidates as landforms to be implemented in adaptation strategies in Haiti and the larger Caribbean region.

Experimental and observational studies have shown mangroves' capacity to abate the flooding impacts of storm surges by reducing water elevation and velocity due to drag in their complex root systems. Field observations of storm surges created by Category 3 Hurricane Wilma along the Gulf Coast of South Florida showed effective attenuation of storm surges by the Everglades mangroves, with the surge amplitudes decreasing by a rate of up to 40-50 cm/km across the forest (Zhang et al., 2012). An experiment using scale models of mangroves by Maza et al. (2017) indicates reductions in the velocity field by up to 50 percent and turbulence kinetic energy increases by up to fivefold within the root zone compared to upstream conditions. And while it is hard for numerical simulations to accurately quantify mangrove forests' storm surge attenuation property, hydrodynamic modeling studies have demonstrated their attenuating effect on storm surge amplitudes and flood durations (Montgomery et al., 2019; Chen et al., 2021). Mangroves' ability to restrict water flow across the forest width then leads to reductions in peak water levels, flooding extent, and flood duration in areas within and behind the forest.

At the same time, the degree to which mangroves are effective in providing coastal protection depends on their health and cover, which are influenced by environmental processes. Hydrodynamic properties, such as tidal patterns and hydroperiod, play a role in the propagation and zonation of mangroves (Crase et al., 2013; Salas-Rabaza et al., 2023). Salinity levels, closely linked with hydrodynamics, play an essential role in the well-being of mangroves, as prolonged high salinity exposure may result in restricted growth of trees (Krauss et al., 2008) and has been shown to be the primary contributor behind several mangrove diebacks around the world (Lagomasino et al., 2021; Lovelock et al., 2017). Other identified environmental factors influencing mangrove health include temperature, light, nutrients, and sediment supply. Consequently, climate events like droughts or long-term phenomena such as sea-level rise may threaten mangrove forests' health and resilience.

Before assessing the potential of current mangrove covers in the Caribbean as natural infrastructure, it is essential to evaluate how their recent health has changed due to stressors related to climate and human activities. Remote Sensing tools and techniques are well suited to answer this question as they offer frequent data points on ecosystems and landforms, letting observers track these systems' evolution over time and their response to external factors or events. Examples include the monitoring of crop growth and health (Sadeh et al., 2021) , monitoring the resilience of mangroves to sea level rise (Duncan et al., 2018) and measuring their biophysical characteristics (Jean-Baptiste & Jensen, 2006). Hence the use of satellite imagery has been shown to be appropriate for studying mangroves. Tools such as machine learning and vegetation indices can be used to track the extent and health of mangrove forests over time. Coupled with other climate data, these time series can help us determine the impacts of climate events on these forests.

In this paper, we develop and apply a workflow to assess and track mangrove forest health over the last decade. Satellite images of mangrove forests in Haiti taken between 2010 and 2020 are classified and analyzed to distinguish mangrove covers from other land covers. This lets us measure their extent evolution through indices and metrics that reflect forest health. This analysis then allows us to quantify changes in mangrove health in Haiti, helping us understand the relationship between their resilience and recent climate events.

2 Data and Study Sites

The Grand-Pierre Bay mangrove forest, located at the mouth of the Artibonite Valley, was selected for this study due to its significant size (largest single mangrove extent in Haiti), and proximity to population and economic centers.

Satellite imagery from PlanetLabs' RapidEye archive is used for our analysis. With a 5m pixel resolution, this satellite lets us better distinguish smaller-scale forest cover details than other satellites such as Landsat (30m resolution). PlanetLabs also provides high temporal resolution with near-daily observations, letting us follow seasonal changes in our sites. While featuring fewer bands than Landsat for analysis, the provided 5-band imagery (Red, Blue, Green, RedEdge, and Near-Infrared) is still well-suited to land classification, particularly when used in conjunction with indices such as the Normalized Difference Vegetation Index (NDVI) and the Normalized Difference Water Index (NDWI). As such, intra-annual observations are taken between 2010 and 2020 at the Grand-Pierre Bay site. Cloud cover permitting, several observations are taken in a single month. With a decade-long observation period, we can observe seasonal and inter-annual patterns of mangrove health and cover.

Baie de Grand-Pierre, Haiti (Grand-Pierre Bay)

Figure 1. The Grand-Pierre Bay mangrove forest (outlined in solid white) is located on the Central coastline of Haiti, South of the city of Gonaives. The major rivers' paths (La Quinte, L'Estère and Artibonite) are highlighted. Major settlements are outlined in dashed lines.

The Grand-Pierre Bay Mangrove Forest (outlined in white in Fig.1) is located south of Gonaives, the 3rd most populated city in Haiti, in the Artibonite department. It is the largest single extent of mangroves in Haiti and is fed by the La Quinte and L'Estère rivers, the two most important rivers in this department after the Artibonite River. The mangrove forest sits seaward of a lagoon, acting as a buffer for parts of the Artibonite Valley coastline. Its close proximity to Gonaives and the Artibonite Valley mouth is significant as this region houses one of the largest disadvantaged urban populations of the country, with the commune of Gonaives holding the largest number of people living in income poverty in Haiti in 2012 (Pokhriyal et al., n.d.). The Artibonite Valley is also one of the country's most important agricultural production regions, with over 70 percent of the country's rice production, a local staple, occurring in the valley ("Assessing the Potential Impact of Climate Change on Rice Yield in the Artibonite Valley of Haiti Using the CSM-CERES-Rice Model", n.d.).

Caroni Swamp, Trininad-and-Tobago

Figure 2. Caroni Swamp (outlined in solid white) is located on the Western coast of the island of Trinidad, South of the cities of Port-of-Spain and San Juan.

To ground-truth the analyses that we present below, which focus on Grand-Pierre Bay, we require independent observations of land cover in order to train the land classification model. The primary site providing this data is the Caroni Swamp (outlined in white in Fig. 2), which is located south of the capital city of Trinidad and Tobago, Port-of-Spain. It is the country's largest mangrove wetland, protected under the Ramsar Convention for International Wetland Protection. The swamp is home to numerous channels, lagoons, and intertidal mudflats. Unlike the chosen Haitian sites, the Caroni Swamp is surrounded by highly urbanized areas, with Port-of-Spain and San Juan to the north and Chaguanas to the southeast and built infrastructure backing the mangrove on its landward edge. This site is used for ground-truthing our land classification model.

2.1 Climate Forcing during Observation Period

Rainfall estimates from the Climate Hazards Group InfraRed Precipitation with Station data (CHIRPS) are used to follow climate trends in the Grand-Pierre Bay mangrove forest over our observation period (Fig. 14). CHIRPS is a 35+ year quasi-global rainfall data set which combines interpolated station data and gridded satellite-based precipitation estimates from NASA and NOAA (Funk et al., 2015).

Additionally, tide gauge data from around the island of Haiti/Hispaniola (across Haiti and the Dominican Republic) are used to monitor the local sea level variations (Fig. 15).

3 Methods

Our approach involves using remote sensing indices (defined below) to support the classification of images and the calculation of metrics to be analyzed.

3.1 Indices

Normalized Difference Water Index - NDWI

The Normalized Difference Water Index (NDWI) assesses the presence and extent of surface water bodies. It is used here to mask the open water pixels surrounding the mangrove forest to aid the land classification process. This is done using the Green and Near-Infrared bands, following the relation defined by McFeeters (1996):

$$NDWI = \frac{Xgreen - Xnir}{Xgreen + Xnir}$$

Our land classification and analysis uses the land surfaces obtained after masking out open water using NDWI based on a threshold of 0.2, with values higher than this threshold masked as open water.

Normalized Difference Vegetation Index - NDVI

The Normalized Difference Vegetation Index (NDVI) is a simple indicator of green vegetation's presence, density, and health. This index uses the Near-Infrared and Red bands of observations as follows:

$$NDVI = \frac{Xnir - Xred}{Xnir + Xred}$$

Applied to our mangrove cover after masking it out from other land covers, we gauge the density and health evolution of our mangroves through time series and looking at the spatial difference of NDVI distribution between 2020 and 2010:

$$dNDVI = NDVI_{2020} - NDVI_{2010}$$

3.2 Land Classification using Machine Learning

Unsupervised Learning

Initially, we explored employing unsupervised learning to quickly determine what features and structures can be found and classified from our images and surface reflectance data. The unsupervised classified images helped us familiarize ourselves with the sites' likely covers and distributions. This analysis was conducted using the K-means clustering algorithm, popular for image segmentation (Ikotun et al., 2023). This method initializes k centroids (where k is the user-defined number of clusters). The centroids are then recomputed as the mean of all the data points in the cluster, and the assignment of data points to clusters is repeated until the centroids no longer change or a stopping criterion is met. For land classification, K-means clustering can group pixels in an image based on spectral properties, such as their reflectance values in different bands. It can identify different land cover types in an image by grouping similar pixels, such as water, vegetation, and urban areas.

We used this method on the surface reflectance values to classify the land cover into four groups, which we then associated with open water, mangrove vegetation, viable land, and bare soil (mud flat). The viable land classification refers to pixels containing either low-density vegetation or bare soil fit for colonization by mangroves. After masking out the open water and bare soil covers, the remaining mangrove vegetation and viable land covers were compared over the years to track the patterns in mangrove cover change and are considered in our supervised analysis. While K-means clustering is a quick method of classifying land cover, we found that it was not sufficiently accurate for our classifications, and it produced inconsistent results within and across observations. As such, we instead use a supervised method for our analysis, as outlined in the next section.

Figure 3. Ground truthing points and classifications from Caroni Swamp, Trinidad and Tobago.

Supervised Learning

Supervised learning is a machine learning paradigm for classifying objects using a set of input objects such as a vector of variables and their desired or human-labeled ("supervised") outputs to train a model. This model can then be used to classify or predict the output of other similar input objects. In a remote sensing context, this set of input objects or training data may look like geolocated points or polygons containing pixels labeled as a certain land cover type or classification. The spectral values of the pixel(s) contained at the point or polygon are then associated with a given category. This is particularly useful here as we can control the classification scheme and make use of ground truthing to validate our models. We used supervised learning to classify the pixels of our satellite imagery into different land type categories, letting us distinguish and track different land cover types systematically. While unsupervised classification methods such as K-means clustering can also be used for land classification on single observations, they lack the higher accuracy and re-usability of supervised methods, which lets us reuse the same trained model on unseen data, giving us a tool to classify land on newly acquired satellite images continuously.

For this study, we use ground-truthing data from the mangroves found in Caroni Swamp, Trinidad and Tobago. The data was collected during a two-day field outing where the locations of different land cover classes were recorded using a Garmin GPSMAP 78sc device. The data comprises 98 data points across the forest (as seen in Figure 3), and is made of the following classes: open water, mangroves, mudflat, intertidal zone, urban, and crops/other vegetation. The data is split in a 70-30 ratio, with 70 percent of the labels randomly selected to be part of the training set and the remaining 30 for our model's testing validation set. In addition to the training set from the Caroni Swamp field cam-

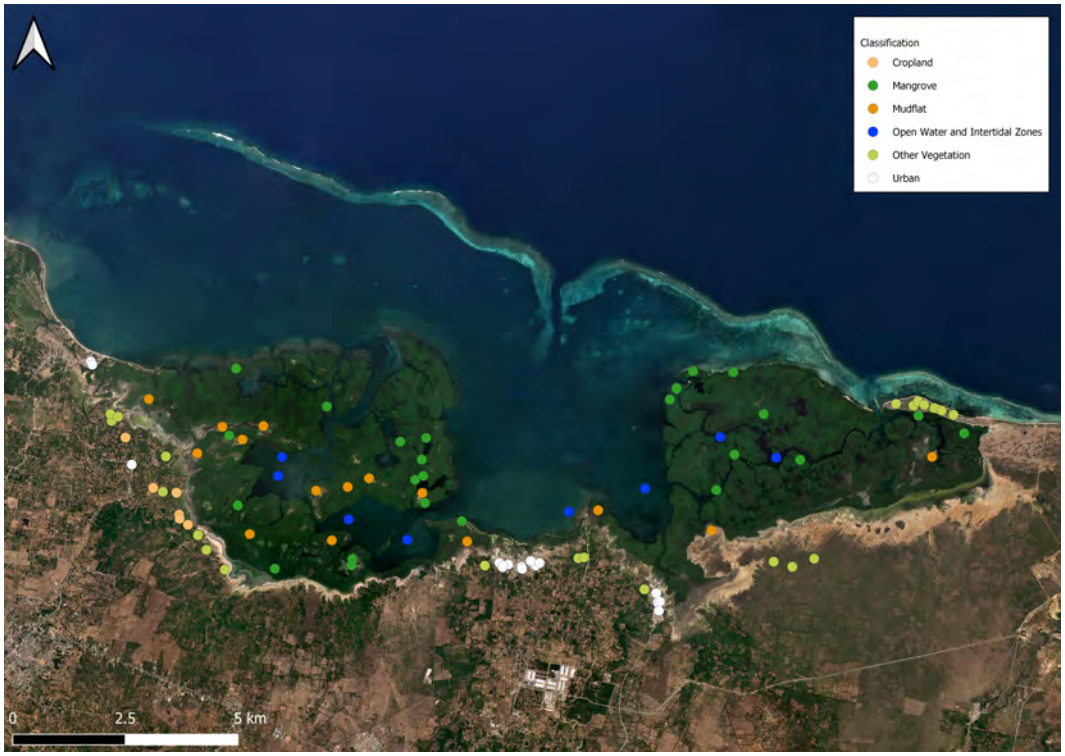

Figure 4. Additional model training points from Caracol Bay, Haiti

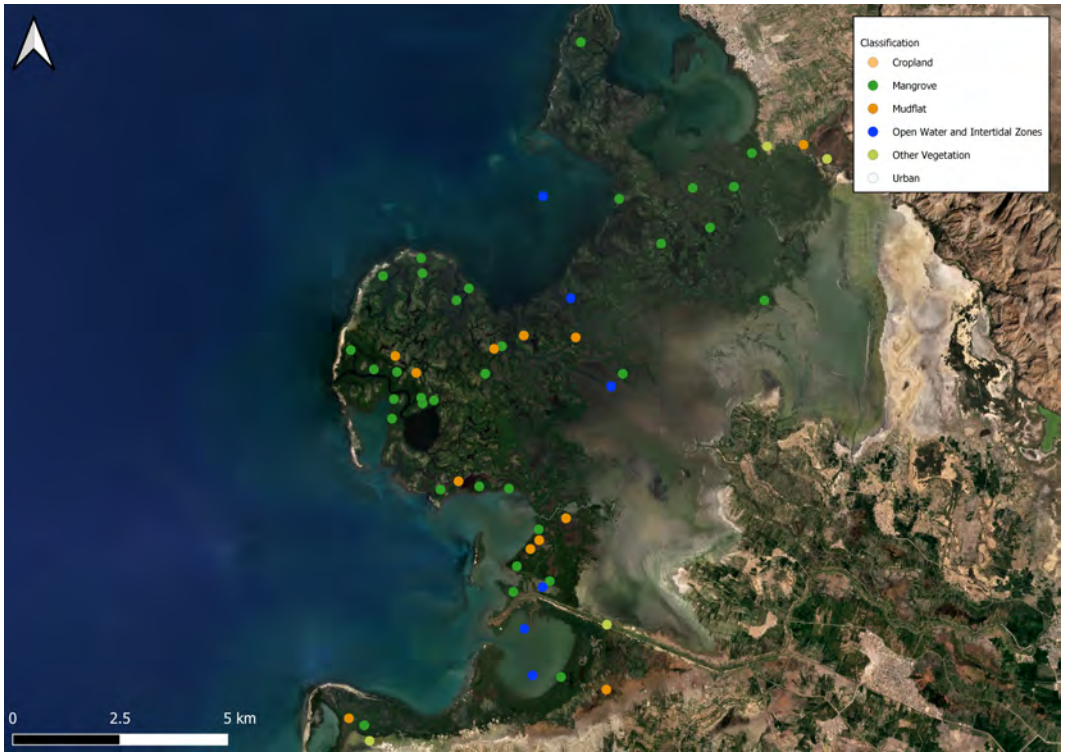

Figure 5. Additional model training points from Grand-Pierre Bay, Haiti

paign, training data points from other mangrove sites in Haiti, namely in Grand-Pierre Bay (Fig. 5) and Caracol Bay (Fig. 4) were also used. These points and their labels were identified using an initial unsupervised classification and confirmed using visual imagery of the sites. As such, while our training set was taken both from this remote identification and ground truths in Caroni Swamp, the validation is exclusively composed of ground truth data points in Caroni Swamp. Using a model trained with this data across Caribbean sites is appropriate here as the tracked ecosystems and landforms are similar, with the same mangrove tree species and land cover types being found across the studied sites.

The algorithm used for our land classification is the Histogram-based Gradient Boosting Classifier (referred to as HGB hereafter) provided in the scikit-learn Python library. HGB is an implementation of the Light Gradient Boosting Machine (LightGBM) framework (Ke et al., 2017) , a widely-used machine learning solution using tree-based learning algorithms and favored for its' fast training speed, low memory usage, and accuracy. LightGBM (and the HGB implementation) was chosen over other machine learning of for its' native support for missing values (NaNs) which would undermine our workflow, as NaN's arise from clouds and any open water pixels that are removed from our images. We use HGB to classify land cover based on the pixels' reflectance values in different bands. The identified mangrove pixels are then masked, isolated, and used in our analysis with vegetation indices to quantify the mangrove forest cover and extent changes as laid out in the following workflow.

Model Validation

Because the classifications made by the model are estimations, we use bootstrapping to conduct its validation. Bootstrapping is a resampling technique where we create multiple new datasets by randomly sampling subsets of the original dataset with replacement. By taking samples from our original dataset and training and evaluating the model multiple times, we can better assess the model's performance variability and robustness.

Results from validation of the trained model on randomly sampled ground-truthed points in Caroni Swamp, Trinidad and Tobago, show robust model performance. This is conducted by resampling, classifying and testing randomly sampled points from the validation set in a bootstrap process, with the data being resampled 800 times. Testing a sample point involves checking whether the classification from the model matches the observed classification from ground-truthing.

To assess the model's performance, we look at the distribution of the mean classification accuracies for each resampling step during the bootstrap process within a 95 percent confidence interval. With this process, we find with model accuracies falling within a 91.4 and 95.9 percent range (Fig. 6). While this shows high general model accuracy, we are also interested in class-based accuracies. The confusion matrix pictured in Fig. 7 A. shows the prediction accuracies for each class in the main diagonal, while the off diagonals show what each class is misclassified as and the ratio of misclassifications. We see a range between 84 and 96 percent for the predicted classes, with the lowest being crops and the highest being mangroves. While the percentage of misclassified crop pixels seems significant - with 3.9% misclassified as urban, 4.3% as mangroves and 8.1% as open water - the total number of misclassified pixels during the bootstrapping process (as seen in Fig. 7B. with the unnormalized matrix) are dwarved by the total number of correctly classified urban, mangroves and open water pixels. As we are principally interested in the cover of mangroves and unvegetated areas of the forest, such as mudflats, we have concluded the model to be robust and appropriate enough for the sake of this analysis.

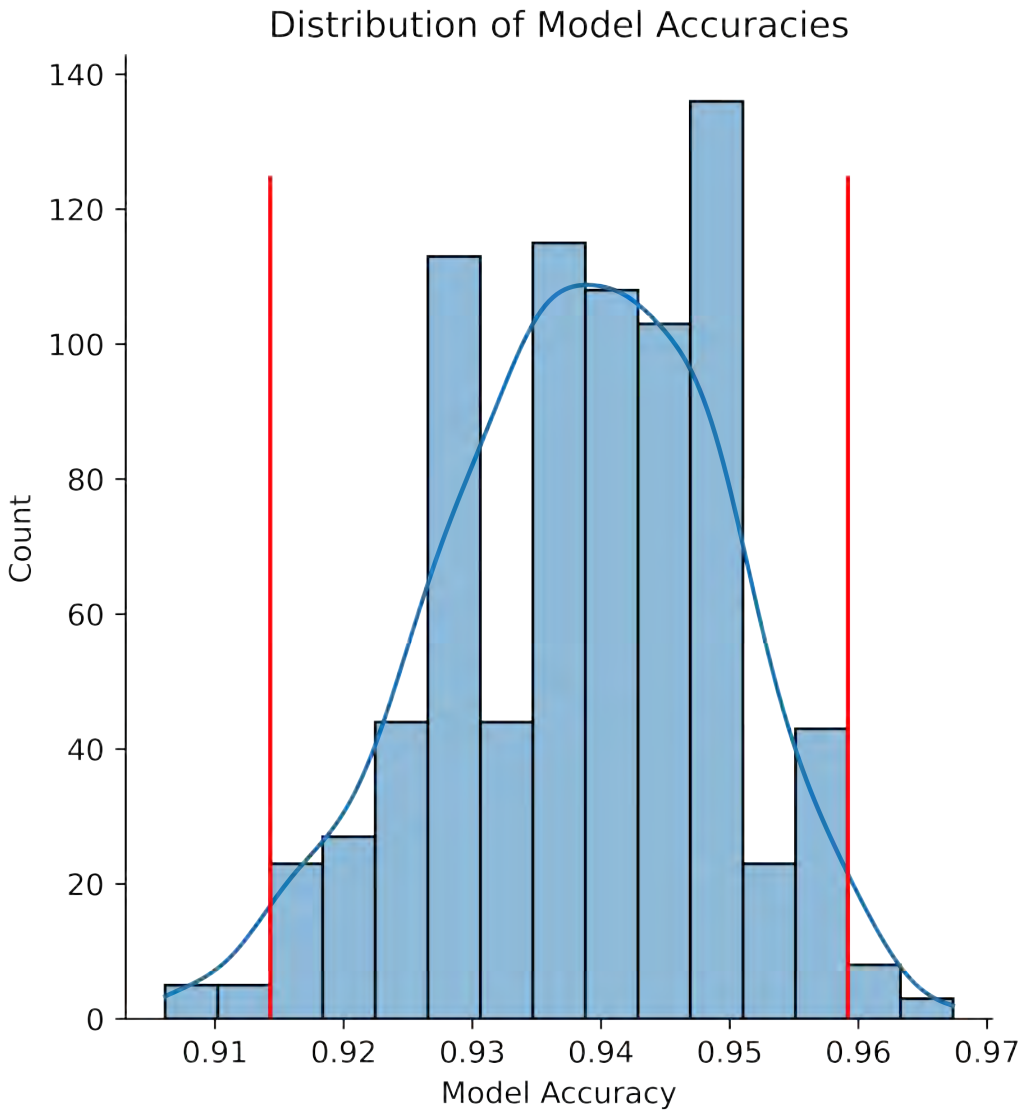

Figure 6. Distribution of Model Accuracies from Bootstrapped Validation Runs.

3.3 Workflow

Our workflow started with acquiring and preprocessing satellite images for which the land cover was classified. We retained the mangrove and mudflat classes for our analysis of the classified land cover types. These classes and the NDVI band in our imagery were used to create products such as time series, metrics, and maps for our analysis. The different components of this workflow (pictured in Fig. 8) and their interactions are outlined in the following subsections.

Preprocessing Images

Images obtained from Planet's archive are screened based on cloud cover, with observations presenting less than 10 percent of cloud cover being retained for analysis. This leaves us with 45 images between 2010 and 2020. Unfortunately, no images were found to be suitable in 2017, as well as the 2011, 2019, and 2020 Wet seasons. While these gaps

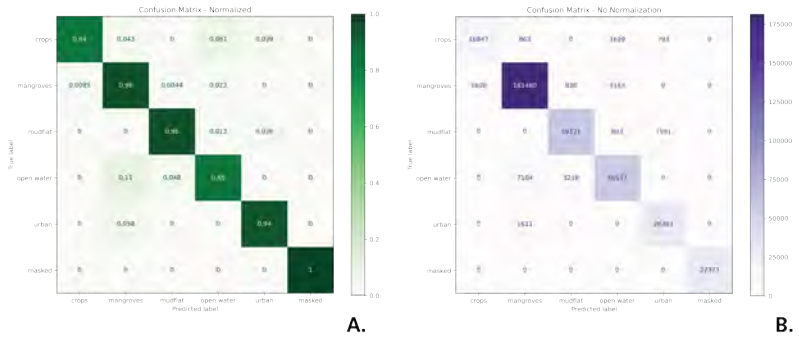

Figure 7. Confusion Matrix of Predicted vs. True Labels of the classification model on Caroni Swamp ground truth points. A. Normalized confusion matrix. B. Unnormalized confusion matrix.

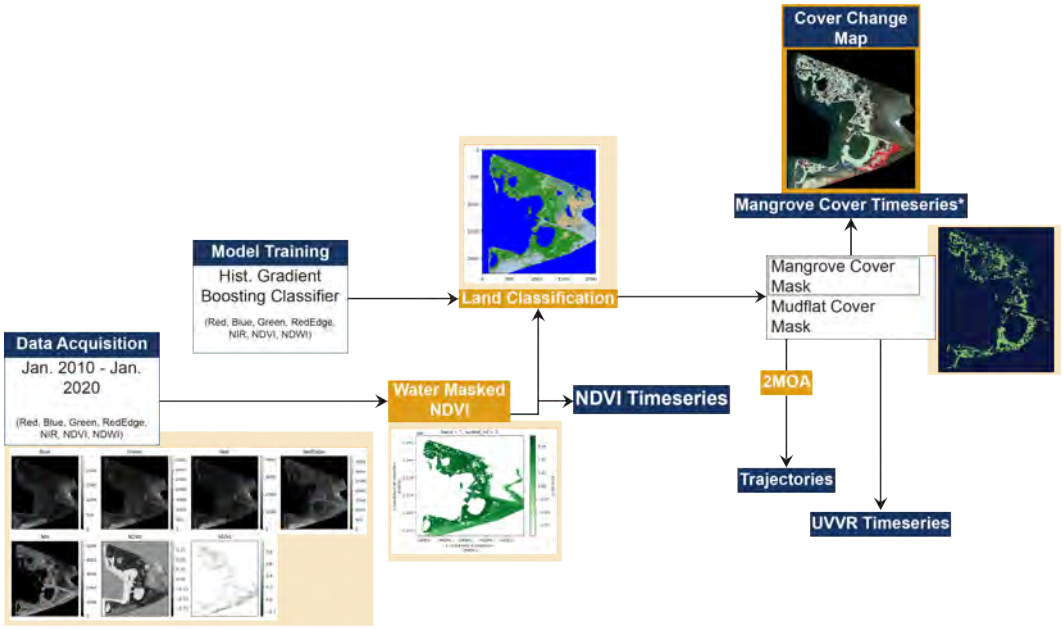

Figure 8. Methods and Tools Workflow

in the data may mean losing some of the finer details of mangrove health progression, we can still make out the overall trends in the 2010 to 2020 period.

Before they are used for either model training or classification of images, the satellite images are preprocessed by masking the open water and urban areas using the NDVI and NDWI indices (defined below). This masking relies on thresholds in these two indices, with NDWI larger than or equal to 0.2 indicating open water pixels and NDVI lower than or equal to 0.2 indicating urban/non-vegetated pixels. Masking open-water and urban areas significantly reduces the complexity of these covers for the model, making it more accurate at predicting these categories.

Model Training and Selection

Following preprocessing, reflectance values across bands are sampled at the locations of our training and validation data points. The hyperparameters of our model were tuned using a grid search, and particular attention was given to the band weights. Be-

cause bands and layers such as RedEdge, NIR, and NDVI are good at detecting and distinguishing vegetation from other cover types (Gandhi et al., 2015), as well as stress within vegetation (Boiarskii & Hasegawa, 2019), we give them a higher class weight in our model. The final parameters used can be found in the Appendix.

Land Classification and Postprocessing

Once the model trained and selected, we used it to classify the 45 observations from Grand-Pierre Bay. From the classified images (featuring open water, mangroves, mudflat, intertidal zone, urban, and crops/other vegetation categories), we created new maps featuring mangrove vegetation and unvegetated regions (by combining mudflats and intertidal zones), leaving us with maps containing only the perceived extents of the mangrove forest by excluding urban, open water, crops, and other vegetation categories. These new maps were then used to compute the metrics defined below on the vegetated and unvegetated sections of the forest.

3.4 Metrics

Gross Cover Change

The gross cover change of mangroves for a given site is the first metric we use to track physical changes in the wetland. While it does not tell us anything about forest density and spatial distribution of vegetation, it is an easy-to-calculate metric for a high-level understanding of how the mangrove evolves. The gross cover of a single observation is calculated by counting the number of pixels classified as mangroves and multiplying that number by the resolution of a single pixel, as provided by the specifications of the utilized satellite instrument. The Gross Cover Change is then the difference in gross mangrove cover between the two observation dates.

Unvegetated to Vegetated Ratio - UVVR

The Unvegetated to Vegetated Ratio is an index that helps establish vegetation cover status and track wetland changes (Couvillion et al., 2021). It does so by taking the ratio of unvegetated pixels (such as mud flats) to the vegetated pixels (like mangroves in our case). The closer to zero our UVVR, the more vegetation there is in our site and the more dense this forest is. At values of UVVR above 1.0, the forest has significant regions of unvegetated, exposed soil. As such, increases in UVVR over time indicate loss of mangrove forest, which could be due to natural disasters, changes in environmental conditions, or deforestation due to human activity. Conversely, decreases in UVVR denote afforestation. We implement this simple relation as follows for each observation:

$$UVVR = \frac{\#mangrove}{\#mudflats + \#intertidalzone}$$

where # is the "number of pixels of."

4 Results and Discussion

Our analysis of forest health dynamics in Grand-Pierre Bay then revolves around the spatio-temporal changes in NDVI values within the mangrove vegetation pixels, as identified by our supervised classification algorithm and their distribution. The NDVI observations are sorted and aggregated per seasons and years. Haiti presents 2 distinct seasons: wet and dry, with the wet season going from April to October, and the dry season going from November to March.

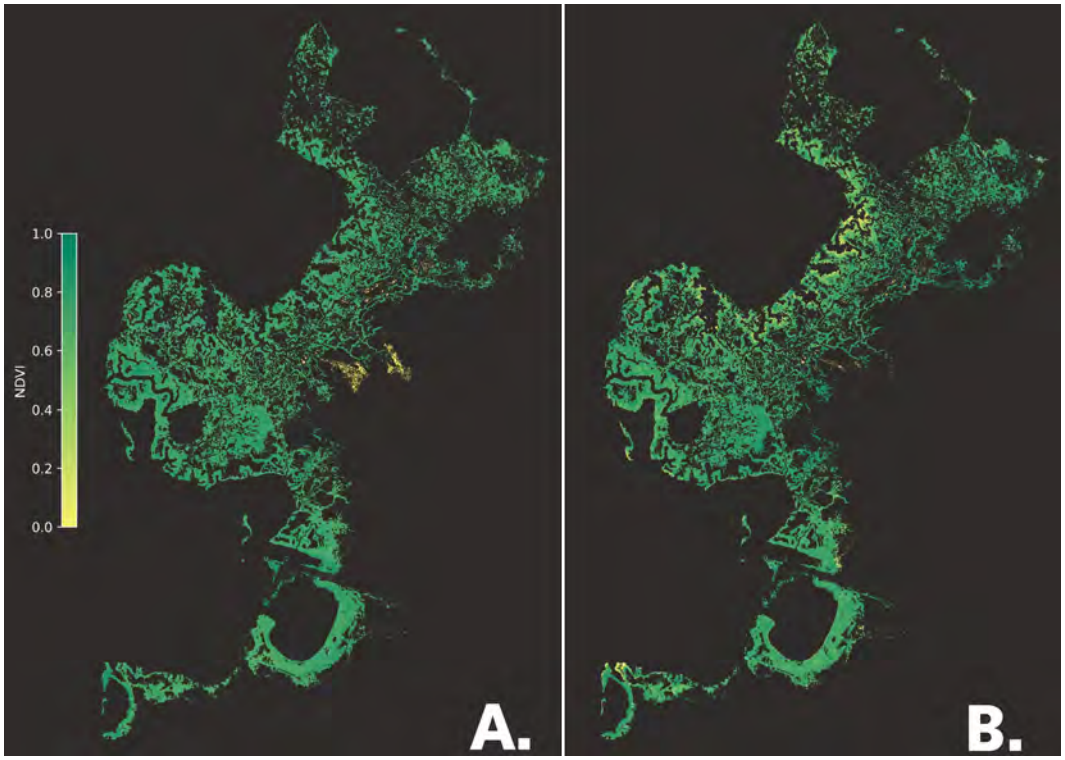

Figure 9. Aggregated mangrove pixels and their NDVI values. A. Mangrove cover and NDVI in 2010. B. Mangrove cover and NDVI in 2020.

4.1 Change in NDVI

To capture and analyze the spatial changes in mangrove health, we use and compare the aggregated pixels classified as mangroves and their NDVI values in 2010 and 2020 (Fig. 9). Displayed in those images are the pixels classified as mangroves for each year, as well as the NDVI values within them. The yellow colors stand out as locations where forest health is suffering, and the difference between 2010 (left) and 2020 (right) can most strikingly be seen along the seaward edge, with the 2020 image showing deteriorating forest health along its boundary.

By formally taking the difference in NDVI values between the aggregated data for the years 2010 and 2020 (dNDVI), we can identify and map pixels in the 2020 cover with decreases and increases in NDVI, with negative dNDVI values signifying reduced vegetation health or death, and positive values signifying increased health or growth. As seen in Figure 10, the forest includes regions of decline and growth. This pattern here is displayed in terms of percentage change for a given pixel. While the change can have larger magnitudes than 100 percent, we limit the scale to +100 and -100 for a better visualization of the spatial distribution of change; with NDVI values of vegetation generally ranging between 0.2 and 1, the death of mangroves is seen as sharp declines from the vegetation range into values close to zero or negatives as cover transitions to bare soil/mud and open water. Conversely, new growth and establishments display sharp increases in NDVI values into the vegetation range. Because NDVI varies between -1 and 1, these sharp changes frequently create relative changes larger than 100 percent (i.e., a pixel with a positive value in 2010 could be negative in 2020). Displaying the full range of percent change then puts a highlight on the deaths and new growths of mangroves,

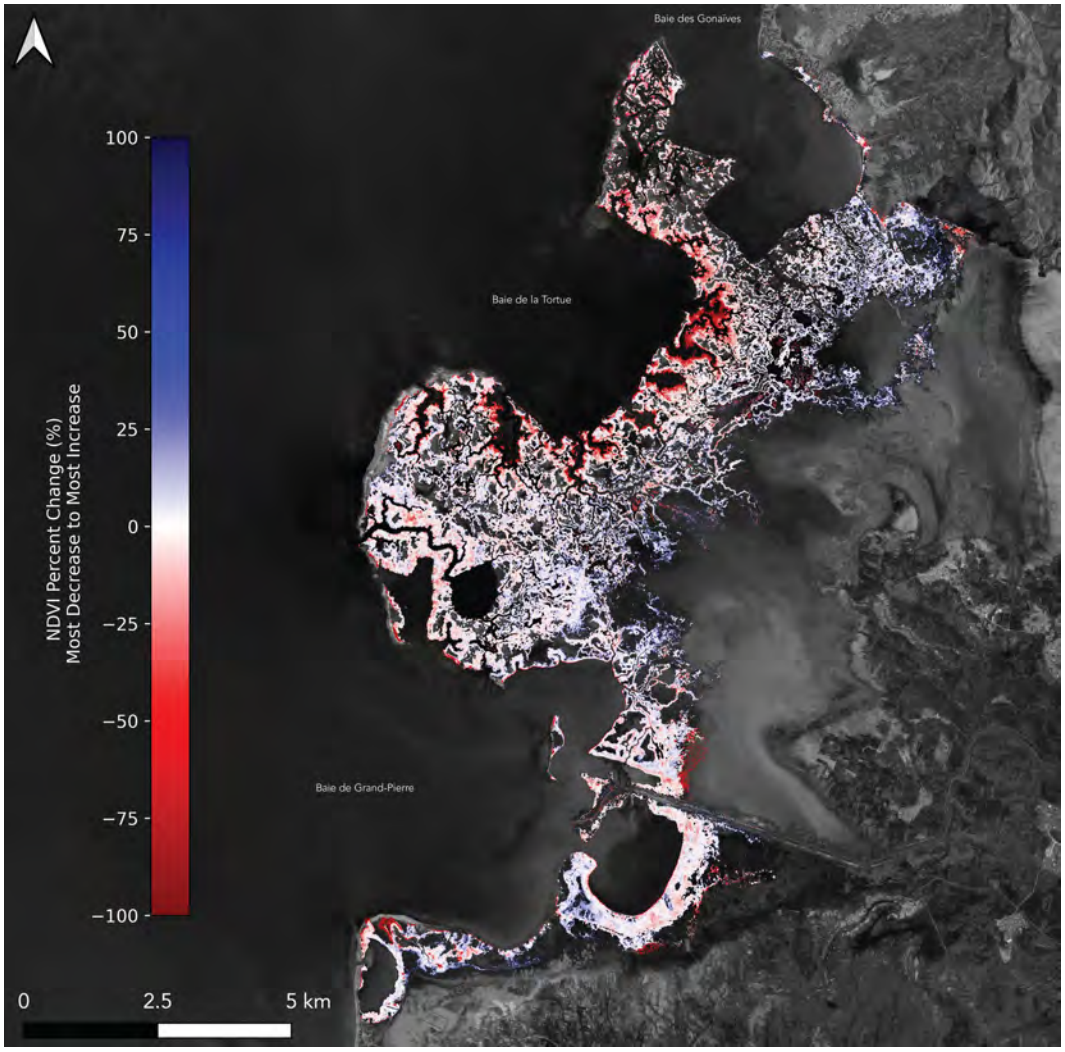

Figure 10. Change in NDVI within mangrove cover between 2020 and 2010.

while losing the finer details of decreasing and increasing health in perpetuating mangroves.

The declines are concentrated in the sea-facing areas (seaward), particularly in the central embayment of our site in Baie de la Tortue, while pockets of growth appear in the lagoon and land-facing areas (landward). This spatial distribution indicates a landward retreat of the forest. With areas showing declines in NDVI of 100 percent and more, indicating the possible death of vegetation, the forest is experiencing diebacks on its coastal front, while having renewed health and growth next to the lagoon.

4.2 Mangrove Cover Change

Similarly, we use the 2010 and 2020 aggregated mangrove covers (pixels classified as mangrove) to capture the change in mangrove cover. Through comparison with the 2010 land cover classification, we identify pixels in the 2020 land cover classification in which mangrove was lost (the pixel was classified as mangrove in 2010, but not in 2020), mangrove was gained (was not mangrove in 2010, but was in 2020), and remained the same (was classified as mangrove in both 2010 and 2020). This mangrove cover change

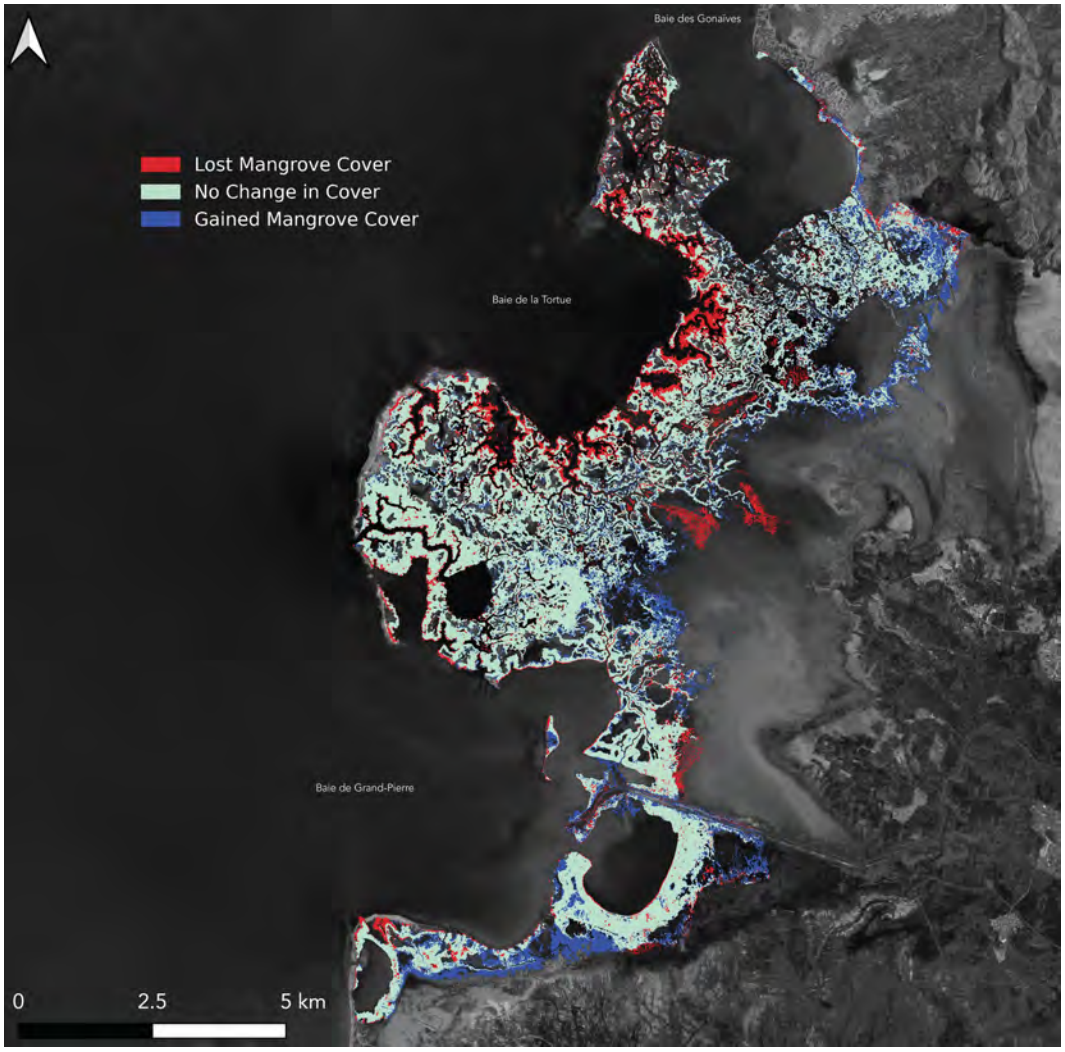

Figure 11. Change in mangrove cover between 2010 and 2020.

map (Fig. 11) shows areas of mangrove retreat and new growth. The spatial change in NDVI showed strong health declines seaward, and increases landward. This is corroborated by the change in mangrove cover, with systematic retreat seen seaward, particularly around Baie de la Tortue, while new growth is seen across the landward boundary of the forest.

The changes in mangrove health across the forest were stark enough to trigger diebacks and also change the forest's cover composition. Using the change in detected mangrove cover, we observe reduced mangrove cover mainly in the Baie de la Tortue between 2010 and 2020. Following the gross mangrove cover and UVVR progression and their year-to-year percent change in Table 1, we see a sharp decline in mangrove cover and UVVR in 2013, followed by a timid and varied recovery of mangrove cover, most likely driven by new growth landward of the forest. While there was a strong initial recovery of cover and UVVR in 2014, this recovery stalls in 2017, and the forest cover and ratio of vegetation to unvegetated did not recover to pre-2013 levels, implying that while the forest showed some resilience, it displays a net loss of cover, and the recovery and landward migration of cover did not keep up with the continued loss on the coastline.

Table 1. Mangrove Cover and UVVR Evolution

Year	Mangrove Cover (km^2)	Percent Change	UVVR	Percent Change
2010	198.688	–	1.065	–
2011	200.989	1.158	1.091	2.513
2012	211.319	5.139	1.192	9.216
2013	187.708	-11.173	0.985	-17.360
2014	195.841	4.333	1.060	7.643
2015	198.585	1.401	1.058	-0.186
2016	201.019	1.226	1.098	3.729
2017	195.354	-2.818	1.013	-7.731
2018	198.919	1.825	1.061	4.760
2019	190.856	-4.054	0.947	-10.784
2020	196.018	2.705	0.983	3.802

With this new growth landward within the lagoon and intertidal zones, the Grand-Pierre Bay mangrove forest is effectively migrating landward and retreating from the coastline. This process is unfortunately unsustainable, as it appears that even over the 10-year observation period, the landward progression of the mangrove was insufficient to offset the loss of forest on its seaward edge. Additionally, there is the question of space, as not all of the intertidal zone may be suitable for new establishments, and that space is limited. This has implications for the coastal defense properties of this mangrove forest in the future that will need to be further studied to better assess its role in the coastal protection of this region.

4.3 Spatio-Temporal Change in the Forest

This pattern of decline and growth in the forest was not a constant spatial or temporal process. In Fig. 12 , stacked ridge plots show the seasonal variation of NDVI values found in the forest across the observation period. NDVI values from all observations are aggregated per season, wet and dry, across the decade of observations, with each ridge displaying the distribution of values for each season. A look at seasonal NDVI distributions within the mangrove forest, while having alternating trends pre-2013, shows a consistent decrease in mangrove health after the 2013 dry season. This decline slows down in 2016, with distributions having smaller left tails and lower upper bounds 2018 forward. This move and change in the distributions may indicate a reorganization in the forest structure. This restructuring of the forest would hint at an underlying environmental process driving this redistribution of cover.

Two possible candidates are sea-level rise and changes in climate and precipitation. Between 2013 and 2015, Haiti suffered through the unprecedented Pan-Caribbean drought, which heavily impacted precipitations, freshwater outflows, and precipitation-evapotranspiration balance in the region (Herrera et al., 2018). Precipitation estimates from CHIRPS show a sharp decline in wet season precipitations in the Artibonite region. Figure 14, which displays the distribution of precipitations in wet and dry seasons from 2000 to 2021 water years, features a strong decline between 2013 and 2016, with lower means and heavy precipitation in both the wet and dry seasons, confirming lower precipitation and freshwater inputs in the forest.

Coincidentally, tide gauge data around the island of Haiti showcase rises in local sea level between 2010 and 2015, followed by a decrease between 2015 and 2017 (Fig. 15). While the lack of long-term, continuous tidal data in the region makes it hard to characterize regional sea-level rise, this local variation in sea-level across the island indicates possible sea and wave action stressors on the coastline of the mangrove forest.

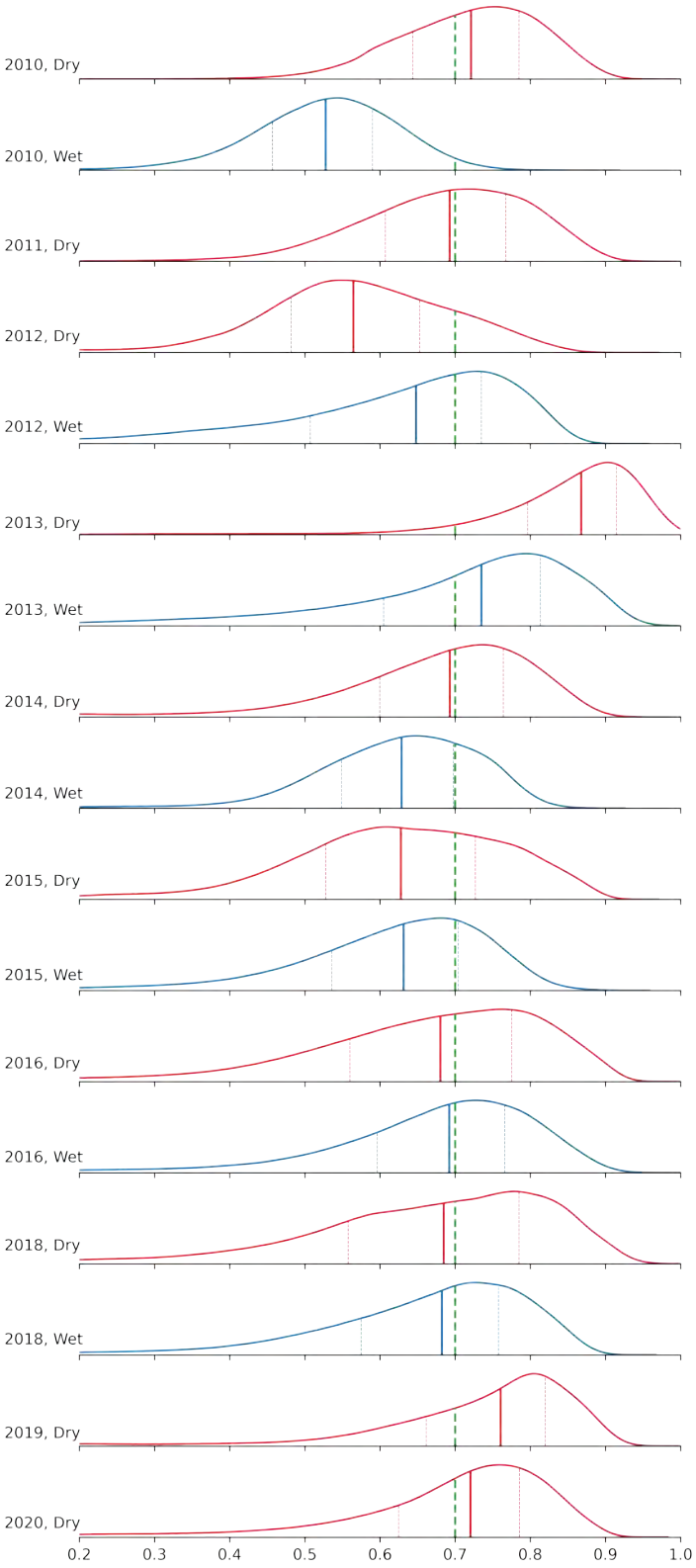

Figure 12. Seasonal Distribution of NDVI values within mangrove cover in Grand-Pierre Bay. The green dotted line represents the NDVI threshold for healthy vegetation (NDVI = 0.7).

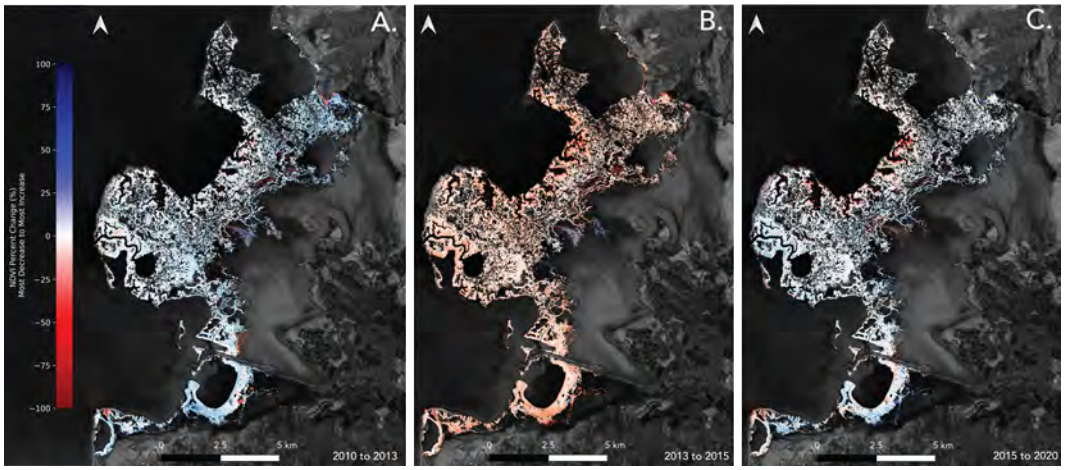

Figure 13. Progression of NDVI changes during the 2010 decade. A. Features the pre-drought changes (2010-2013). B. Features change during the drought period (2013-2015). C. Features post-drought changes (2015-2020).

This change in structure can be seen by looking at the time progression of spatial change in forest health. (Fig. 13) shows the spatial change in NDVI between the following three periods: pre-drought 2010-2013 (Fig. 13A.), drought 2013-2015 (Fig. 13B.), and post-drought 2015-2020 (Fig. 13C.). While some light decline can be seen in the Baie de la Tortue, the forest sees increases in NDVI in most locations. The 2013-2015 drought period saw a uniform decline in the forest, most accentuated in coastal-facing areas. The post-drought recovery of the forest is, however, not uniform, with the decline continuing in the coastal facing regions and light increases in NDVI occurring in the landward regions. Looking at these three periods, we observe that the Pan-Caribbean drought coincides with an acceleration of the seaward loss of mangroves.

We hypothesize that the reduced freshwater inputs from the drought likely raised the salinity levels in the forest, leaving mangroves more vulnerable to sea action and other environmental stressors. A review on the environmental drivers of mangrove establishment and early development by (Krauss et al., 2008) frames temperature, light, flooding, salinity, and nutrients as the major ecophysiological health factors for this critical life stage of mangroves. While we were not able to acquire observations of local temperature or light changes, it is safe to say that the combined effects of drought and rising local sea levels would disrupt flooding regimes, freshwater inputs, and nutrient inputs from rivers. These disruptions would potentially raise salinity levels in the forest, decrease nutrient inputs, and expose the coastal front of the forest. The spatial variability in mangrove health and cover change is then most likely the result of the combined actions of regional sea-level rise on weakened mangrove trees in low-lying areas farthest from river outflows, which were likely most impacted by high salinity during the drought, leading to diebacks, and more difficult reestablishment in the same areas.

5 Conclusions

A sharp decline in mangrove cover and health was observed during the 2013-2016 Haitian drought, followed by a spatially heterogeneous recovery, with most of it occurring on the landward area of the forest and continued retreat happening along its seaward edge, particularly along the shore of Baie de la Tortue (Fig. 1). This indicates resilience to environmental stressors in the forest, but not an equal one; as the forest re-

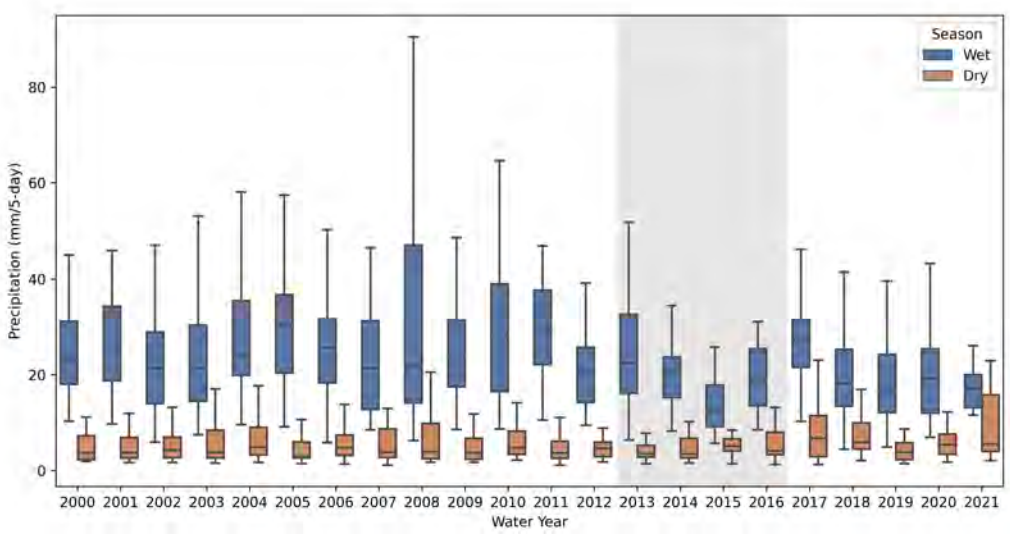

Figure 14. Estimated Precipitation Distributions in the Artibonite Region. Estimations are generated by ClimateEngine.org through the CHIRPS dataset (2000-2020).

covers from lowered freshwater inputs and local rises in sea-level, the forest migrates landward. This landward migration is unsustainable, as it may not be able to occur fast enough to keep up with the increased frequency and severity of climate change induced environmental stressors, and as not all of the available space landward is suitable for mangrove establishment.

To ensure the continuation of the protection benefits of this mangrove forest, targeted conservation and restoration efforts may be needed on forest's most vulnerable regions on the coastline, while supporting the further establishment of mangroves landward. Based on these new understandings of how mangrove forest may evolve under climate forcing, future work may include hydrodynamic studies to quantify the change in protection services offered by this landform. Only with an integrated consideration of how the ecology and the climate forcing evolve can we achieve a resilient future that makes most effective use of these natural protective features.

Open Research Section

Rainfall estimates can be accessed from the Climate Hazard Center database at UC Santa Barbara via the ClimateSERV online toolkit: `https://climateserv.servirglobal.net`. To obtain the data, follow the "Getting Started" link, then upload a zipped shapefile of the Artibonite River Watershed as an Area of Interest (AOI). This file is available in the project's GitHub repository under `datasets/Shapefiles/Artibonite_AOI.zip`. Next, select "Observation" as the Data Type, choose "UCSB CHIRPS Rainfall" as the Data Source, set the Calculation to "Average," and specify a date range from 01/01/2000 to 12/31/2020. Ensure that you "Add Query" and then "Submit Query." After processing, the dataset will be available for download as a .csv file.

Alternatively, the raw precipitation raster files are accessible in the CHIRPS dataset directory at `https://data.chc.ucsb.edu/products/CHIRPS-2.0`. Monthly rainfall estimates for the Caribbean are available in the `camer-carib_monthly` directory, while global daily estimates can be found in the `global_daily` directory. Using the AOI, mean daily precipitation can be derived for the same time period.

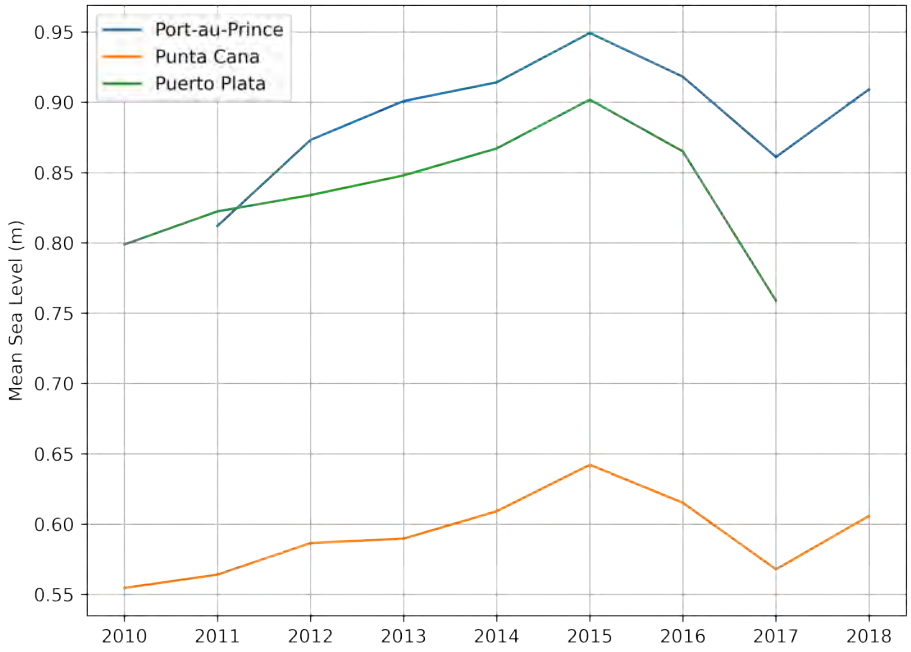

Figure 15. Yearly mean sea levels from tide gauge data in Haiti and the Dominican Republic.

Tidal gauge data in Port-au-Prince, Punta Cana and Puerto Plata are hosted by the University of Hawaii Sea Level Center and can be accessed through GESLA (Global Extreme Sea Level Analysis) (Haigh et al., 2021), (Woodworth et al., 2016), (Caldwell et al., 2015): `https://gesla787883612.wordpress.com/downloads/`

All processed satellite imagery, data products and supporting data can be accessed from this project's GitHub page: `https://github.com/aesgeorges/MangroveCaribRS`

Acknowledgments

I would like to extend my gratitude to Hearts to Humanity (H2H8), whose generous support enabled the successful carryout of this work. I am thankful for the support of my colleagues and faculties in the Environmental Fluid Mechanics and Hydrology group at UC Berkeley and their constructive feedback. Likewise, inputs from Jean Wiener of FoProBim was invaluable to the shaping of the scope of this project. Finally, I'd like to express my deepest gratitude to my parents, my sister, friends from Haiti and elsewhere, and Claire, who saw me at every step of this project.

References

Assessing the Potential Impact of Climate Change on Rice Yield in the Artibonite Valley of Haiti Using the CSM-CERES-Rice Model. (n.d.). Retrieved 2024-07-01, from `https://doi.org/10.13031/trans.13868`

Boiarskii, B., & Hasegawa, H. (2019, November). Comparison of NDVI and NDRE Indices to Detect Differences in Vegetation and Chlorophyll Content. *JOURNAL OF MECHANICS OF CONTINUA AND MATHEMATICAL SCI-*

ENCES, *spl1*. doi: 10.26782/jmcms.spl.4/2019.11.00003

Caldwell, P., Merrifield, M. A., & Thompson, P. R. (2015). *Sea level measured by tide gauges from global oceans — the Joint Archive for Sea Level holdings (NCEI Accession 0019568), Version 5.5.* NOAA National Centers for Environmental Information. Retrieved 2024-08-19, from http://doi.org/10.7289/V5V40S7W (Last Modified: 2024-07-29) doi: http://doi.org/10.7289/V5V40S7W

Chen, Q., Li, Y., Kelly, D. M., Zhang, K., Zachry, B., & Rhome, J. (2021, October). Improved modeling of the role of mangroves in storm surge attenuation. *Estuarine, Coastal and Shelf Science*, *260*, 107515. Retrieved 2023-11-20, from https://www.sciencedirect.com/science/article/pii/S0272771421003668 doi: 10.1016/j.ecss.2021.107515

Couvillion, B., Ganju, N. K., & Defne, Z. (2021). *An Unvegetated to Vegetated Ratio (UVVR) for coastal wetlands of the Conterminous United States (2014-2018).* U.S. Geological Survey. Retrieved 2024-08-05, from https://www.sciencebase.gov/catalog/item/5fa18656d34e198cb793cba5 doi: 10.5066/P97DQXZP

Crase, B., Liedloff, A., Vesk, P., Burgman, M., & Wintle, B. (2013, July). Hydroperiod is the main driver of the spatial pattern of dominance in mangrove communities. *Global Ecology & Biogeography*, *22*. doi: 10.1111/geb.12063

Duncan, C., Owen, H. J. F., Thompson, J. R., Koldewey, H. J., Primavera, J. H., & Pettorelli, N. (2018). Satellite remote sensing to monitor mangrove forest resilience and resistance to sea level rise. *Methods in Ecology and Evolution*, *9*(8), 1837–1852. Retrieved 2022-05-24, from https://onlinelibrary.wiley.com/doi/abs/10.1111/2041-210X.12923 (_eprint: https://onlinelibrary.wiley.com/doi/pdf/10.1111/2041-210X.12923) doi: 10.1111/2041-210X.12923

Funk, C., Peterson, P., Landsfeld, M., Pedreros, D., Verdin, J., Shukla, S., ... Michaelsen, J. (2015, December). The climate hazards infrared precipitation with stations—a new environmental record for monitoring extremes. *Sci Data*, *2*(1), 150066. Retrieved 2024-08-19, from https://www.nature.com/articles/sdata201566 (Publisher: Nature Publishing Group) doi: 10.1038/sdata.2015.66

Gandhi, G. M., Parthiban, S., Thummalu, N., & Christy, A. (2015, January). Ndvi: Vegetation Change Detection Using Remote Sensing and Gis – A Case Study of Vellore District. *Procedia Computer Science*, *57*, 1199–1210. Retrieved 2024-08-05, from https://www.sciencedirect.com/science/article/pii/S1877050915019444 doi: 10.1016/j.procs.2015.07.415

Haigh, I. D., Marcos, M., Talke, S. A., Woodworth, P. L., Hunter, J. R., Hague, B. S., ... Thompson, P. (2021, November). GESLA Version 3: A major update to the global higher-frequency sea-level dataset. Retrieved 2024-08-19, from https://eartharxiv.org/repository/view/2828/ (Publisher: EarthArXiv)

Herrera, D. A., Ault, T. R., Fasullo, J. T., Coats, S. J., Carrillo, C. M., Cook, B. I., & Williams, A. P. (2018). Exacerbation of the 2013–2016 Pan-Caribbean Drought by Anthropogenic Warming. *Geophysical Research Letters*, *45*(19), 10,619–10,626. Retrieved 2024-07-13, from https://onlinelibrary.wiley.com/doi/abs/10.1029/2018GL079408 (_eprint: https://onlinelibrary.wiley.com/doi/pdf/10.1029/2018GL079408) doi: 10.1029/2018GL079408

Ikotun, A. M., Ezugwu, A. E., Abualigah, L., Abuhaija, B., & Heming, J. (2023, April). K-means clustering algorithms: A comprehensive review, variants analysis, and advances in the era of big data. *Information Sciences*, *622*, 178–210. Retrieved 2024-07-02, from https://www.sciencedirect.com/science/article/pii/S0020025522014633 doi: 10.1016/j.ins.2022.11.139

Jean-Baptiste, N., & Jensen, J. R. (2006, December). Measurement of Mangrove Biophysical Characteristics in the Bocozelle Ecosystem in Haiti Using ASTER Multispectral Data. *Geocarto International*, *21*(4), 3–8. Retrieved 2023-11-30, from https://doi.org/10.1080/10106040608542397 (Publisher: Taylor & Francis _eprint: https://doi.org/10.1080/10106040608542397) doi: 10.1080/10106040608542397

Ke, G., Meng, Q., Finley, T., Wang, T., Chen, W., Ma, W., ... Liu, T.-Y. (2017). LightGBM: A Highly Efficient Gradient Boosting Decision Tree. In *Advances in Neural Information Processing Systems* (Vol. 30). Curran Associates, Inc. Retrieved 2024-10-17, from https://papers.nips.cc/paper_files/paper/2017/hash/6449f44a102fde848669bdd9eb6b76fa-Abstract.html

Krauss, K. W., Lovelock, C. E., McKee, K. L., López-Hoffman, L., Ewe, S. M. L., & Sousa, W. P. (2008, August). Environmental drivers in mangrove establishment and early development: A review. *Aquatic Botany*, *89*(2), 105–127. Retrieved 2023-09-26, from https://www.sciencedirect.com/science/article/pii/S0304377008000089 doi: 10.1016/j.aquabot.2007.12.014

Lagomasino, D., Fatoyinbo, T., Castañeda-Moya, E., Cook, B. D., Montesano, P. M., Neigh, C. S. R., ... Morton, D. C. (2021, June). Storm surge and ponding explain mangrove dieback in southwest Florida following Hurricane Irma. *Nat Commun*, *12*(1), 4003. Retrieved 2023-11-06, from https://www.nature.com/articles/s41467-021-24253-y (Number: 1 Publisher: Nature Publishing Group) doi: 10.1038/s41467-021-24253-y

Lovelock, C. E., Feller, I. C., Reef, R., Hickey, S., & Ball, M. C. (2017, May). Mangrove dieback during fluctuating sea levels. *Sci Rep*, *7*(1), 1680. Retrieved 2023-11-06, from https://www.nature.com/articles/s41598-017-01927-6 (Number: 1 Publisher: Nature Publishing Group) doi: 10.1038/s41598-017-01927-6

Maza, M., Adler, K., Ramos, D., Garcia, A. M., & Nepf, H. (2017, November). Velocity and Drag Evolution From the Leading Edge of a Model Mangrove Forest. *Prof. Nepf via Elizabeth Soergel*. Retrieved 2023-11-20, from https://dspace.mit.edu/handle/1721.1/119430 (Accepted: 2018-12-04T19:54:28Z Publisher: American Geophysical Union (AGU))

Montgomery, J. M., Bryan, K. R., Mullarney, J. C., & Horstman, E. M. (2019). Attenuation of Storm Surges by Coastal Mangroves. *Geophysical Research Letters*, *46*(5), 2680–2689. Retrieved 2023-11-20, from https://onlinelibrary.wiley.com/doi/abs/10.1029/2018GL081636 (_eprint: https://onlinelibrary.wiley.com/doi/pdf/10.1029/2018GL081636) doi: 10.1029/2018GL081636

Murakami, H., Delworth, T. L., Cooke, W. F., Zhao, M., Xiang, B., & Hsu, P.-C. (2020, May). Detected climatic change in global distribution of tropical cyclones. *Proceedings of the National Academy of Sciences*, *117*(20), 10706–10714. Retrieved 2022-05-13, from https://www.pnas.org/doi/10.1073/pnas.1922500117 (Publisher: Proceedings of the National Academy of Sciences) doi: 10.1073/pnas.1922500117

Pokhriyal, N., Zambrano, O., Linares, J., & Hernández, H. (n.d.). Estimating and Forecasting Income Poverty and Inequality in Haiti.

Sadeh, Y., Zhu, X., Dunkerley, D., Walker, J. P., Zhang, Y., Rozenstein, O., ... Chenu, K. (2021, April). Fusion of Sentinel-2 and PlanetScope time-series data into daily 3 m surface reflectance and wheat LAI monitoring. *International Journal of Applied Earth Observation and Geoinformation*, *96*, 102260. Retrieved 2023-10-03, from https://www.sciencedirect.com/science/article/pii/S030324342030903X doi: 10.1016/j.jag.2020.102260

Salas-Rabaza, J. A., Reyes-García, C., Méndez-Alonzo, R., Us-Santamaría, R., Flores-Mena, S., & Andrade, J. L. (2023, December). Hydroperiod modulates early growth and biomass partitioning in Rhizophora man-

gle L. *Aquatic Botany*, 103747. Retrieved 2023-12-25, from https://www.sciencedirect.com/science/article/pii/S0304377023001328 doi: 10.1016/j.aquabot.2023.103747

Woodworth, P. L., Hunter, J. R., Marcos, M., Caldwell, P., Menéndez, M., & Haigh, I. (2016). Towards a global higher-frequency sea level dataset. *Geoscience Data Journal*, *3*(2), 50–59. Retrieved 2024-08-19, from https://onlinelibrary.wiley.com/doi/abs/10.1002/gdj3.42 (_eprint: https://onlinelibrary.wiley.com/doi/pdf/10.1002/gdj3.42) doi: 10.1002/gdj3.42

Zhang, K., Liu, H., Li, Y., Xu, H., Shen, J., Rhome, J., & Smith, T. J. (2012, May). The role of mangroves in attenuating storm surges. *Estuarine, Coastal and Shelf Science*, *102-103*, 11–23. Retrieved 2022-05-24, from https://www.sciencedirect.com/science/article/pii/S0272771412000674 doi: 10.1016/j.ecss.2012.02.021